Chemical Geology 417 (2015) 356–370

Contents lists available at ScienceDirect

Chemical Geology

journal homepage: www.elsevier.com/locate/chemgeo

Assessing compositional variability and migration of natural gas in the Antrim Shale in the Michigan Basin using noble gas geochemistry

Tao Wen [a,*], M. Clara Castro [a], Brian R. Ellis [b], Chris M. Hall [a], Kyger C. Lohmann [a]

[a] University of Michigan, Department of Earth and Environmental Sciences, Ann Arbor, MI 48109-1005, USA
[b] University of Michigan, Department of Civil and Environmental Engineering, Ann Arbor, MI 48109-2125, USA

ARTICLE INFO

Article history:
Received 14 August 2015
Received in revised form 15 October 2015
Accepted 18 October 2015
Available online 19 October 2015

Keywords:
Antrim Shale gas
Noble gases
Groundwater recharge
Biogenic methane
Thermogenic methane
Sedimentary basins

ABSTRACT

This study uses stable noble gases' (He, Ne, Ar, Kr, Xe) volume fractions and isotopic ratios from Antrim Shale natural gas to assess compositional variability and vertical fluid migration within this reservoir, in addition to distinguishing between the presence of thermogenic versus biogenic methane. R/Ra values, where R is the measured $^{3}He/^{4}He$ ratio and Ra is the atmospheric value of $1.384 \pm 0.013 \times 10^{-6}$, vary from 0.01 to 0.34 suggesting a largely dominant crustal ^{4}He component with minor atmospheric and mantle contributions. Crustal ^{21}Ne, ^{40}Ar and ^{136}Xe contributions are also present but the atmospheric component is largely dominant for these gases. Crustal contributions for ^{21}Ne, ^{40}Ar and ^{136}Xe vary between 1.1% and 12.5%, between 0.7% and 19% and between 0.1% and 2.7%, respectively. A few samples present higher than atmospheric $^{20}Ne/^{22}Ne$ ratios pointing to the presence of a small mantle Ne component. High horizontal and vertical variability of noble gas signatures in the Antrim Shale are observed. These are mainly due to variable noble gas input from deep brines and, to a smaller extent, variable in-situ production within different layers of the Antrim Shale, in particular, the Lachine and Norwood members. Estimated ^{4}He ages, considering external ^{4}He input for Antrim Shale water, vary between 0.9 ka and 238.2 ka and match well for most samples with the timing of the major Wisconsin glaciation, suggesting that Antrim Shale water was influenced by glaciation-induced recharge. Consistency between measured and predicted $^{40}Ar/^{36}Ar$ ratios assuming Ar release temperatures ≥250 °C supports a thermogenic origin for most of the methane in these samples. This thermogenic methane is likely to originate at greater depths, either from the deeper portion of the Antrim Shale in the central portion of the Michigan Basin or from deeper formations given that the thermal maturity of the Antrim Shale in the study area is rather low.

1. Introduction

With rising demands for cleaner domestic energy resources, unconventional hydrocarbon production has been extensively developed since 1979 (Curtis, 2002; Hill and Nelson, 2000; Nicot et al., 2014). As a result, unconventional reservoirs (e.g., black shales) accounted for more than one third of the total natural gas production in the United States in 2013 (US EIA, 2015).

The Antrim Shale in the Michigan Basin has been one of the most actively developed shale gas plays in the USA with its major expansion taking place in the late 1980s (Curtis, 2002; Harrison, 2007; Walter et al., 1996). Unlike most shale gas plays in the USA (e.g., Barnett and Marcellus Shales) (Nicot and Scanlon, 2012), the Antrim Shale is naturally highly fractured (Apotria et al., 1994; Ryder, 1996). It has been suggested that ice sheet advances and retreats enhanced the dilation of preexisting fractures and induced freshwater recharge into the Antrim Shale (McIntosh et al., 2011). This, in turn, supported microbial methanogenesis (Clark, 1982; Martini et al., 1998, 2003; McIntosh and Walter, 2005). Previous natural gas exploitation in the Antrim Shale indicates that natural gas production rates could vary over an order of magnitude suggesting possibly highly localized heterogeneities within the Antrim Shale, particularly within the Lachine and Norwood members (Manger et al., 1991). However, little is known about the relationship between variable natural gas production rates and geochemical composition variability in the Antrim Shale.

Previous studies, located mostly in the northern lower peninsula of Michigan (NPT: Northern Producing Trend) (Figs. 1 and 2A), investigated the origin of the main dissolved solids as well as timing (^{14}C ages) of meteoric recharge into the Antrim Shale (Farrand and Eschman, 1974; Martini et al., 1996, 1998; Walter et al., 1996). Based on methane and co-produced formation waters, a biogenic origin for the majority of the methane was suggested, with thermogenic gas making up <20% of the total produced gas (Martini et al., 1996). However, recent studies have suggested that the contribution of thermogenic methane should be comparable to that of biogenic methane, based on measurement of multiple substituted methane isotopologues ($^{13}CH_3D$, $^{12}CH_2D_2$) (Stolper et al., 2014, 2015). Although identifying the timing of freshwater recharge

* Corresponding author at: Department of Earth and Environmental Sciences, University of Michigan, 2534 C. C. Little Building, 1100 North University Ave., Ann Arbor, MI 48109-1005, USA.
E-mail address: jaywen@umich.edu (T. Wen).

http://dx.doi.org/10.1016/j.chemgeo.2015.10.029
0009-2541/

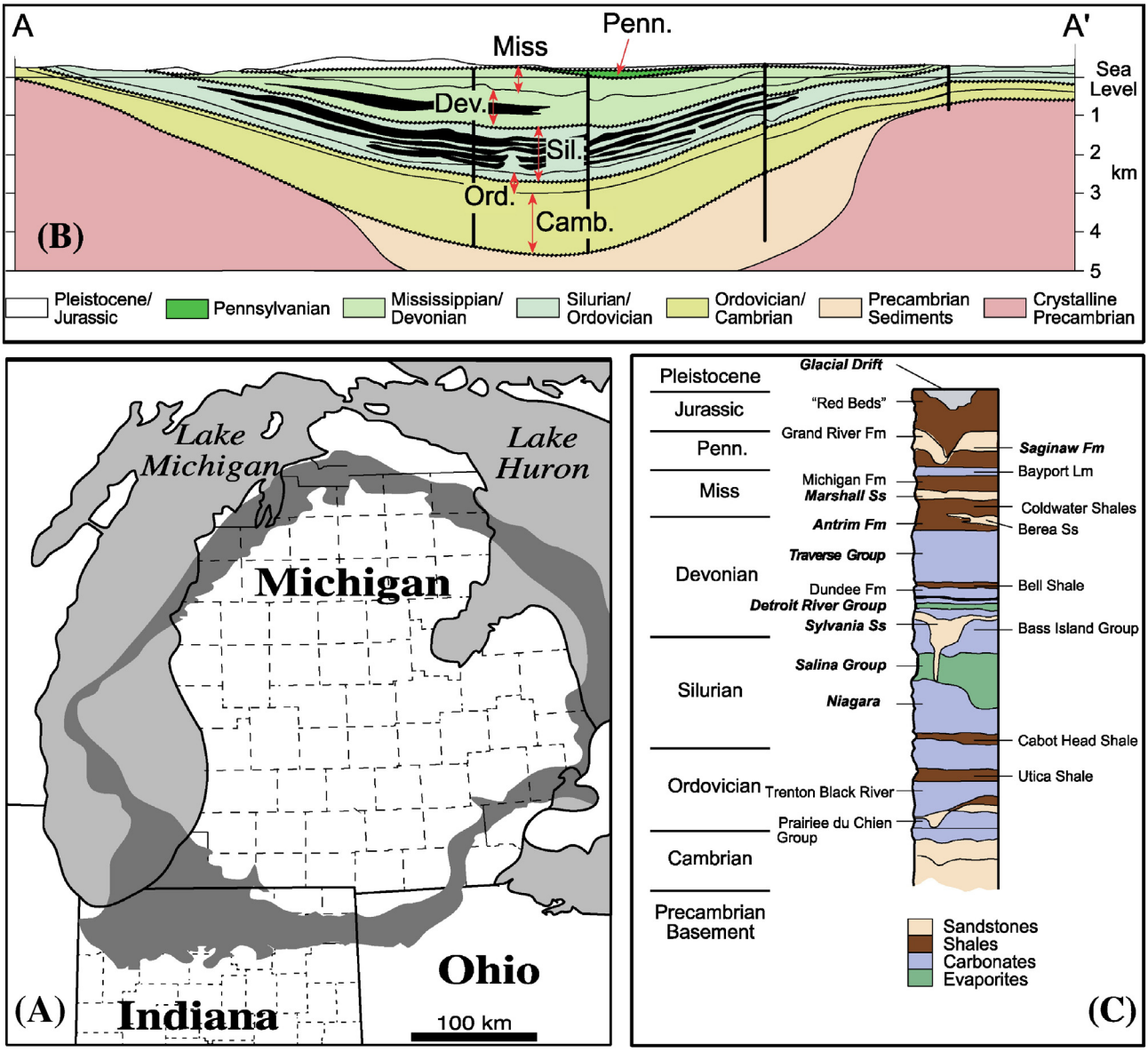

Fig. 1. (A) Central portion of the Michigan Basin (lower peninsula of Michigan). The subcrop of the Antrim Shale is shown in dark brown; the Northern Producing Trend (NPT) of the Antrim Shale gas play is indicated by the rectangular area (adapted from Martini et al., 1998); (B) General schematic geological representation along cross section A–A′ in (a); Rock salts are present in the Michigan Basin as represented by the black layer; (C) Schematic of the Michigan Basin stratigraphy; major formations and lithologies in the basin are identified. (For interpretation of the references to color in this figure legend, the reader is referred to the web version of this article.)

into the Antrim Shale and the relative contribution of thermogenic vs. biogenic methane in Antrim Shale gas can be challenging due to the migration and mixing of waters and gases in the subsurface (Hunt, 1996; Martini et al., 1998; Price and Schoell, 1995; Stolper et al., 2015; Wen et al., 2015), this knowledge is essential to understand the origin, migration and mixing of methane within and beyond the Antrim Shale. Filling these knowledge gaps is important to guide natural gas exploration and to identify the source of methane in the Antrim Shale.

Stable noble gases (Helium — He, Neon — Ne, Argon — Ar, Krypton — Kr, Xenon — Xe) are chemically inert and are thus transported without being affected by chemical reactions or microbial activity (Ballentine, 1991; Hilton and Porcelli, 2003a; Ozima and Podosek, 2002). Moreover, noble gases in subsurface fluids (e.g., freshwater, natural gas) are derived from the atmosphere, crust and mantle, all of which show distinct isotopic and elemental signatures (Hilton and Porcelli, 2003b; Ozima and Podosek, 2002; Pinti et al., 2012; Porcelli et al., 2002). This fact makes noble gases ideal natural tracers for studying the origin and evolution of crustal fluids in sedimentary basins (Ballentine, 1991; Castro et al., 1998a, 1998b; Hilton and Porcelli, 2003b; Kulongoski et al., 2005; Oxburgh et al., 1986; Pinti and Marty, 1995; Warrier et al., 2013). In most subsurface fluids in sedimentary systems, noble gases are dominated by an atmospheric origin (Air Saturated Water or ASW, containing Ne, Ar, Kr and Xe in solubility equilibrium with the atmosphere) and/or crustal components (e.g., $^{4}He^{*}$, $^{21}Ne^{*}$, $^{40}Ar^{*}$, $^{136}Xe^{*}$) where crustal He, Ne, Ar, Kr, and Xe are indicated with the a "*" notation. These result from radioactive decay of U/Th and ^{40}K (Ozima and Podosek, 2002). Mantle contributions are generally minor but not negligible (Castro et al., 2009; Darrah et al., 2014; Ma et al., 2005, 2009a; Pinti and Marty, 2000; Wen et al., 2015).

Previous studies of noble gas isotopic ratios and crustally-produced noble gas components in the shallower Glacial Drift, Saginaw and Marshall aquifers suggest the presence of vertical cross-formational flow (i.e., upward leakage) into these aquifers from deeper formations (Ma et al., 2005; Warrier et al., 2013; Wen et al., 2015). Deep (0.5–3.6 km) brine samples were also collected and analyzed for noble gas concentrations and isotopic ratios in the Michigan Basin and point to

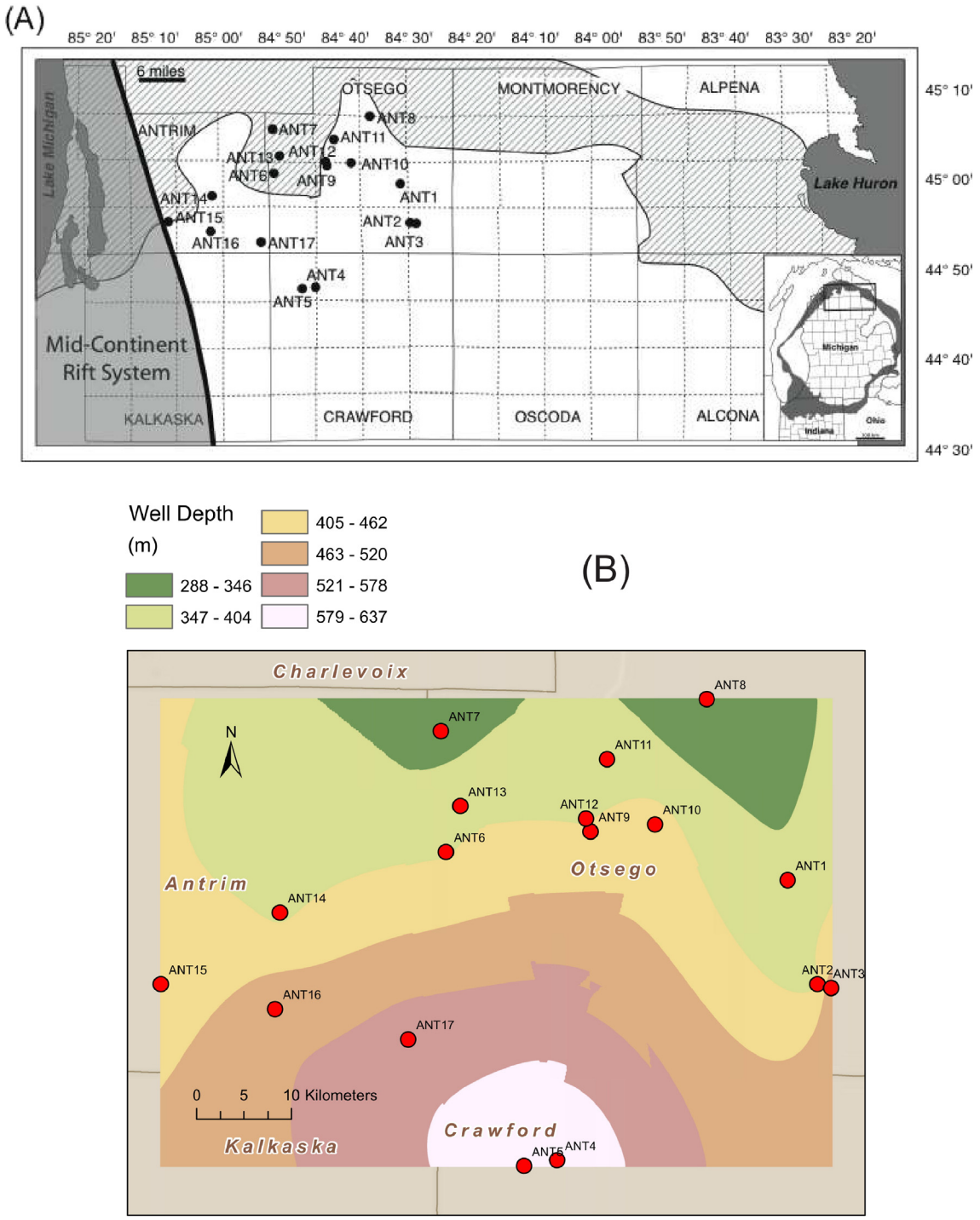

Fig. 2. (A) Location map of all sampled Antrim wells, with Antrim Shale subcrop (stripped area) and Mid-Continent Rift System in the Michigan Basin (black shadow) also indicated; (B) Contour map of perforation depths for sampled Antrim Shale gas wells in this study.

the presence of cross-formational flow (Castro et al., 2009; Ma et al., 2009a). Depletion of atmospheric noble gases in these brines is also observed, indicating the occurrence of a past thermal event in this system (Castro et al., 2009; Ma et al., 2009a, 2009b; Warrier et al., 2013). Such a depletion can be used to identify the contribution of deeper saline formation waters into the Antrim Shale.

In this study, we use noble gas isotopic ratios and volume fractions of natural gas samples from the Antrim Shale to assess the compositional variability of crustally produced noble gases, which would point to variable in-situ production from their parent elements (i.e., U, Th, ^{40}K) and/or the variable contribution of external brines from deeper formations into the Antrim Shale. In addition, ^{4}He ages for Antrim brines are calculated and compared with previously reported ^{14}C ages of Antrim water samples (Martini et al., 1998). We also use ^{40}Ar/^{36}Ar ratios to distinguish between the presence of thermogenic versus biogenic methane in the Northern Producing Trend (NPT) of the Antrim Shale. The Northern Producing Trend, centered near Otsego County, extends to its neighboring counties to the east and west. It is in this area that most of the natural gas producing wells in the Antrim Shale are located.

2. Geologic setting

Located in the northeastern United States, the Michigan Basin is a concentric intracratonic depression floored by crystalline Precambrian basement (Fig. 1), and consists of a succession of sedimentary rocks from Precambrian to Jurassic that reaches depths of over 5 km (Catacosinos and Daniels, 1991; Dorr and Eschman, 1970). The entire sedimentary strata are covered by thick Pleistocene Glacial Drift sediments and are composed mainly of evaporites (e.g., Salina Group), carbonates (e.g., Traverse Formation), shales (e.g., Antrim and Coldwater Formations), and sandstones (e.g., Marshall Formation) (Fig. 1C). Depending on their nature, these sedimentary rocks constitute either aquitards (e.g., shale, evaporites) or aquifers (mostly sandstones and reefal and dolomitized limestones), giving origin to a multi-layered aquifer system (Vugrinovich, 1986; Westjohn and Weaver, 1996). Major tectonic structures such as the Albion-Scipio Fault, the Lucas Fault, and the Howell Anticline are present in southern Michigan and penetrate the Precambrian crystalline basement (Fisher et al., 1988). The Howell Anticline belongs to the Eastern Granite and Rhyolite Province (EGRP), and displays an age of ~1.5 Ga (Hinze et al., 1975; Menuge et al., 2002; Van Schmus, 1992).

The Antrim Shale is a later Devonian formation and consists mainly of black carbonaceous shale. It underlies all of the Mississippian formations and is underlain by the middle Devonian Traverse Group (Apotria et al., 1994; Gutschick and Sandberg, 1991). The circular subcrop of the Antrim Shale is close to the basin margin and underlies the Pleistocene glacial sediments (Fig. 1). From Fig. 2B, which displays contours of perforation depth of the sampled wells, it is apparent that the Antrim Shale deepens from the north to the south. Overall, the Antrim Shale is significantly shallower than other shale gas plays (e.g., Barnett Shale) in the USA, with a perforation depth ranging from 317 to 637 m in the sampling area. The Antrim Shale is divided into four members based on total organic carbon (TOC) content. These members include the Norwood, Paxton, Lachine, and Upper Antrim (Gutschick and Sandberg, 1991), of which the Norwood and Lachine members have the highest organic content (0.5–24 wt.% TOC) and are the main targets of gas exploitation (Martini et al., 1998; Walter et al., 1996). The thermal maturity of the Antrim Shale in the NPT of the Michigan Basin was determined by vitrinite reflectance (R_o) and ranges from 0.4 to 0.6% (Rullkötter et al., 1992), indicating a low level of thermal maturation (preoil generation) (Waples, 1985).

Fractures in the Antrim Shale are regional and were formed during deeper burial (Martini et al., 2003). Two sets of fractures are dominant in the Antrim Shale: (1) NW-striking fractures formed by natural hydraulic fracturing as hydrocarbons were generated near the end of the Alleghenian orogeny, and; (2) NE-striking fractures formed as a result of cooling and unloading during the 1–1.5 km of basin uplift since the Permian (Apotria et al., 1994; Cercone and Pollack, 1991; Ryder, 1996; Wang et al., 1994). The fracture network present in the NPT of the Antrim Shale acts as a reservoir and conduit allowing the migration and mixing of meteoric water from the above Glacial Drift aquifer, and brine from the underlying permeable Traverse limestone (Walter et al., 1996).

The Antrim Shale is somewhat unique among shale gas reservoirs since it produces significant volumes of water and its gas production occurs at relatively shallow depths (~300–600 m below the surface) (Boyer et al., 2006; Dolton and Quinn, 1996); Total average porosity in the Antrim is 9%, and it is assumed that natural gas fills roughly half of this porosity (Curtis, 2002).

3. Sampling and analytical methods

A total of 17 Antrim Shale gas samples were collected at the wellhead of production wells in the NPT area (Fig. 2A, B) in standard refrigeration grade 3/8″ Cu tubes which were then sealed by steel pinch-off clamps (Weiss, 1968). Atmospheric contamination during sampling was minimized by allowing the gas to flush through the system for approximately 5 min. The complete measurement procedure, carried out in the Noble Gas Lab at the University of Michigan, comprises estimation of He, Ne, Ar, Kr, and Xe volume fractions and their respective isotopic ratios, with standard errors for volume estimates of 1.5, 1.3, 1.3, 1.5 and 2.2%, respectively. When replicate analyses are available, an error-weighted average is reported. Analysis procedures are described briefly below.

Shale gas samples in Cu tubes were attached to a vacuum extraction and purification system. The copper tube is connected to a vacuum system at a pressure of ~2×10^{-5} Torr. Once this pressure is achieved and the system isolated from its turbo-molecular vacuum pump, the lower clamp is released to allow gas samples to flow into the extraction and purification section. Dry gas samples are then inlet to a getter with Ti sponge at 600 °C for 5 min to remove all actives gases. Noble gases are then quantitatively extracted and sequentially allowed to enter a Thermo Scientific® Helix SFT mass spectrometer using a cryo-separator. Subsequently, noble gases are trapped onto the cryo-separator at a temperature of ~10 K. The cryo-temperature is subsequently increased sequentially to release temperatures for He, Ne, Ar, Kr, and Xe, at 42 K, 80 K, 205 K, 215 K, and 280 K, respectively. Specifically, at the He release temperature, He is introduced into the mass spectrometer and the signal intensity of ^{4}He is determined for the He concentration estimate. This estimate is then used by the automated system to optimize the amount of He that should be introduced for measurement of the ^{3}He/^{4}He ratio.

Complete measurement procedures involve estimating the concentration of each noble gas component, measuring the isotopic ratios for Ne, Ar, Kr, and Xe, as well as the ^{3}He/^{4}He ratio. First, a portion of a known volume of air is introduced into the molecular sieve section of the extraction system, and all noble gases are measured in turn with the Helix SFT mass spectrometer. This calibrates the mass spectrometer signal size for each noble gas. Subsequent to the air calibration run, the same measurement procedure is performed on a portion of the unknown sample. All noble gas isotopes are measured using a Faraday detector, except for ^{3}He which is measured using an electron multiplier in ion counting mode.

A total of 17 co-produced formation water samples were also collected at the same time for analysis of chloride concentrations (Cl^-). Water samples were filtered with a 0.45 μm Gelman Laboratory AquaPrep filter, and kept in high-density polyethylene bottles with no headspace prior to analysis. Chloride concentrations were determined in the HydroGeochemistry Laboratory at the University of Michigan and were analyzed by ion chromatograph (Dionex DX) with a AS4A column (precision, ±2%). Abundances of major gas components (CH_4, CO_2, N_2) in the produced natural gas samples were collected at the wellheads in stainless steel cylinders and analyzed by Southern Petroleum Laboratories Inc. and Fibertec Environmental Services. Routine methods of gas chromatography were applied to determine the concentrations of CH_4, CO_2 and N_2.

4. Results

4.1. Major gas components in the Antrim Shale gas

Sample names and ID, location, well depth and abundances of major gas components (CH_4, CO_2, N_2) for collected Antrim Shale gas samples are given in Table 1. Locations of all sampled Antrim gas wells are close to the southern boundary of the Antrim subcrop within the NPT region where we may identify the contribution of thermogenic methane in addition to microbial methane (Fig. 2A). This sampling area overlaps also with that of Martini et al. (1998), thus allowing us to compare previous findings by these authors with those of the current study.

Among the major gas components CH_4 (C_1) is largely dominant, ranging from 79.72% to 92.40% by volume and displaying no obvious correlation with depth. CO_2 and N_2 contents are variable and range

Table 1
Well location and major gas components (shown in volume %) for Antrim Shale gas samples.

Sample ID	Well name	County	State	Date	Latitude	Longitude	Depth (m)	CH_4 (%)	CO_2 (%)	N_2 (%)
ANT1	Chester East D3-14	Otsego	MI	12/19/13	44.9881	−84.5135	351	79.73	20.06	0.13
ANT2	State Charlton 4–7	Otsego	MI	12/19/13	44.9180	−84.4851	393	92.40	6.97	0.12
ANT3	Allen Park 9–8	Otsego	MI	12/19/13	44.9154	−84.4721	515	88.09	11.01	0.14
ANT4	St. Frederic X A3-25	Crawford	MI	12/19/13	44.7995	−84.7331	637	–	12.60	–
ANT5	St. Frederic IX B1-26	Crawford	MI	12/19/13	44.7956	−84.7646	607	–	13.16	–
ANT6	Hayes 7 C2-7	Otsego	MI	12/19/13	45.0071	−84.8388	399	80.76	19.18	0.06
ANT7	State Elmira D3-7	Otsego	MI	12/19/13	45.0885	−84.8436	317	91.46	7.68	0.86
ANT8	Dover Ridge A1-5 HDL	Otsego	MI	12/19/13	45.1098	−84.5904	287	92.01	7.20	0.80
ANT9	Bagley 5 D2-5	Otsego	MI	12/19/13	45.0208	−84.7011	415	84.27	15.63	0.10
ANT10	Bagley -Livingston B2-2	Otsego	MI	10/2/14	45.0256	−84.6398	432	79.72	20.18	0.04
ANT11	Livingston A2-21	Otsego	MI	10/2/14	45.0696	−84.6854	376	84.21	15.69	0.10
ANT12	St. Livingston D2-32	Otsego	MI	10/2/14	45.0295	−84.7055	398	84.27	15.63	0.10
ANT13	Camp Ten B3-32	Otsego	MI	10/2/14	45.0379	−84.8252	394	84.07	15.79	0.15
ANT14	Green River C3-26	Antrim	MI	10/2/14	44.9663	−84.9969	393	85.23	13.08	0.11
ANT15	State Custer D1-12	Antrim	MI	10/2/14	44.9180	−85.1100	430	86.51	9.60	0.07
ANT16	Mancelona East A2-23	Antrim	MI	10/2/14	44.9012	−85.0016	504	82.20	11.19	0.14
ANT17	State Mancelona 3–26	Antrim	MI	10/2/14	44.8809	−84.8748	553	79.78	13.80	0.12

Table 2
Noble gas isotopic ratios for Antrim Shale gas samples.

Sample ID	R/R_a	$^{20}Ne/^{22}Ne$	$^{21}Ne/^{22}Ne$	$^{40}Ar/^{36}Ar$	$^{136}Xe/^{130}Xe$	$^{4}He/^{20}Ne$	$^{20}Ne/^{36}Ar$	$^{36}Ar/^{84}Kr$	$\frac{(^{40}Ar/^{36}Ar)_{predicted}}{(^{40}Ar/^{36}Ar)_{measured}}$
ANT1	0.093 ± 0.004	10.35 ± 0.12	0.0304 ± 0.0005	286.4 ± 7.3	2.194 ± 0.023	74 ± 2.4	1.428 ± 0.028	44.6 ± 1	1.11
ANT2	0.022 ± 0.001	9.82 ± 0.49	0.0311 ± 0.0013	298 ± 0.8	2.205 ± 0.021	321 ± 2	0.018 ± 0.001	17 ± 0.3	1
ANT3	0.025 ± 0.003	9.36 ± 0.38	0.0301 ± 0.0011	298.3 ± 0.7	2.179 ± 0.016	230 ± 2	0.013 ± 0.001	22.8 ± 0.5	0.99
ANT4	0.011 ± 0.001	10.08 ± 0.15	0.0316 ± 0.0004	364.1 ± 3.9	2.192 ± 0.012	3099 ± 2	0.205 ± 0.004	11 ± 0.2	1.17
ANT5	0.242 ± 0.006	10.15 ± 0.01	0.0296 ± 0.0002	282.5 ± 0.7	2.123 ± 0.016	3 ± 2	0.773 ± 0.014	71.8 ± 1.4	1.05
ANT6	0.214 ± 0.008	10.14 ± 0.03	0.0331 ± 0.0004	290.1 ± 3.8	2.188 ± 0.024	6 ± 2	0.563 ± 0.011	30.9 ± 0.6	1.02
ANT7	0.034 ± 0.002	9.66 ± 0.04	0.0328 ± 0.0004	296.9 ± 0.7	2.18 ± 0.016	29 ± 2	0.084 ± 0.002	22.3 ± 0.4	1
ANT8	0.047 ± 0.001	10.36 ± 0.26	0.0302 ± 0.001	306.2 ± 4.4	2.177 ± 0.011	93 ± 2	0.199 ± 0.004	9.8 ± 0.2	0.98
ANT9	0.065 ± 0.003	9.78 ± 0.03	0.0324 ± 0.0004	300.1 ± 1.8	2.212 ± 0.018	39 ± 2	0.291 ± 0.005	23.8 ± 0.5	0.99
ANT10	0.233 ± 0.005	9.82 ± 0.12	0.0292 ± 0.0003	298.7 ± 1.6	2.191 ± 0.011	65 ± 2	0.129 ± 0.002	7.1 ± 0.1	0.99
ANT11	0.023 ± 0.002	9.63 ± 0.12	0.0286 ± 0.0005	294.4 ± 0.7	2.235 ± 0.011	84 ± 2	0.038 ± 0.001	35 ± 0.7	1.01
ANT12	0.339 ± 0.006	10.12 ± 0.03	0.0302 ± 0.0003	282.4 ± 2.2	2.165 ± 0.017	3 ± 2	0.728 ± 0.013	50.9 ± 1	1.05
ANT13	0.128 ± 0.004	9.44 ± 0.25	0.0301 ± 0.001	318.8 ± 1.7	2.213 ± 0.014	64 ± 2	0.308 ± 0.009	10.9 ± 0.3	0.94
ANT14	0.104 ± 0.003	10.07 ± 0.25	0.0309 ± 0.0008	305.4 ± 3.3	2.158 ± 0.017	192 ± 2	0.095 ± 0.002	22.1 ± 0.4	0.98
ANT15	0.153 ± 0.003	10.02 ± 0.23	0.0303 ± 0.0007	320.3 ± 5	2.182 ± 0.009	152 ± 2	0.29 ± 0.006	9.8 ± 0.2	0.95
ANT16	0.261 ± 0.005	10.01 ± 0.12	0.0301 ± 0.0004	318.3 ± 4.6	2.173 ± 0.01	64 ± 2	0.514 ± 0.01	10.9 ± 0.2	0.95
ANT17	0.009 ± 0.001	10 ± 0.31	0.0296 ± 0.0008	352.3 ± 1.6	2.175 ± 0.012	846 ± 2	0.256 ± 0.009	8.4 ± 0.3	0.96
Air [a]	1	9.8	0.029	295.5	2.176	0.288	–	–	–

[a] After Ozima and Podosek (2002).

from 6.97% to 20.18% and from 0.04% to 0.15%, respectively. Similarly to CH_4, no obvious correlations are observed between CO_2 and N_2 versus depth (Table 1). However, an inverse correlation is present between CH_4 and CO_2 contents regardless of whether C_1 and CO_2 contents are variable over the sampling area. Because CO_2 is more strongly sorbed initially in the Antrim Shale as pressures continually drop with gas production, a greater percentage of CO_2 is desorbed compared to CH_4 (Martini et al., 2003). This likely explains the observed CH_4 and CO_2 content inverse correlation in this study.

Volume fractions of heavier hydrocarbons (C_{2+}) as well as the carbon isotopic composition of hydrocarbon species are not available for the Antrim gas samples. However, previous geochemical studies in the Antrim Shale have determined the range of $C_1/(C_2 + C_3)$ to vary from 1 to 10,000, strongly suggesting mixing between thermogenic and biogenic gas components within the NPT (Martini et al., 1996, 1998). Methane from the Antrim Shale gas has $\delta^{13}C$ values ranging from −45 to −55‰, straddling typical values of these two gases: thermogenic versus biogenic (Martini et al., 1996). Unusually high $\delta^{13}C$ values of CO_2 co-produced with methane (~ + 22‰) and dissolved inorganic carbon in formation waters (~ + 28%) require a bacterial mechanism (Martini et al., 1998).

4.2. Noble gas signatures in the Antrim Shale gas

Noble gas isotopic ratios (He, Ne, Ar, Kr, Xe) are listed in Table 2. Atmospheric isotopic ratios are also reported for reference.

R/Ra ratios in Antrim Shale gas, where R is the measured $^3He/^4He$ and Ra is the atmospheric ratio value of $1.384 \pm 0.013 \times 10^{-6}$, vary from an almost pure radiogenic (crustal) value of 0.009 ± 0.001 (typical crustal production values are ~0.01–0.05; Oxburgh et al., 1986), to 0.339 ± 0.006 (Fig. 3B). Higher values of measured R/Ra ratios likely indicate the impact of mixing with an atmospheric component (R/Ra = 1) introduced during meteoric recharge. A minor mantle He component is also likely present which may contribute, to a lesser extent, to increased R/Ra ratios. R/Ra values in Mid Ocean Ridge Basalts (MORB) and Ocean Island Basalts (OIB) are ~8 and 50, respectively (Graham, 2002; Starkey et al., 2009). R/Ra values of samples ANT5, ANT6, ANT10, ANT12 and ANT16 are greater than typical crustal values (Table 2 and Fig. 3B).

Fig. 3. Depth profiles of (A) radiogenic ^4He volume fractions, (B) R/R_a ratios, (C) $^{20}Ne/^{22}Ne$ ratios, (D) $^{21}Ne/^{22}Ne$ ratios, (E) $^{40}Ar/^{36}Ar$ ratios and (F) $^{136}Xe/^{130}Xe$ ratios for collected Antrim gas samples revealing high spatial variability of noble gas signatures within the Antrim Shale. Corresponding atmospheric noble gas values are indicated (dashed lines).

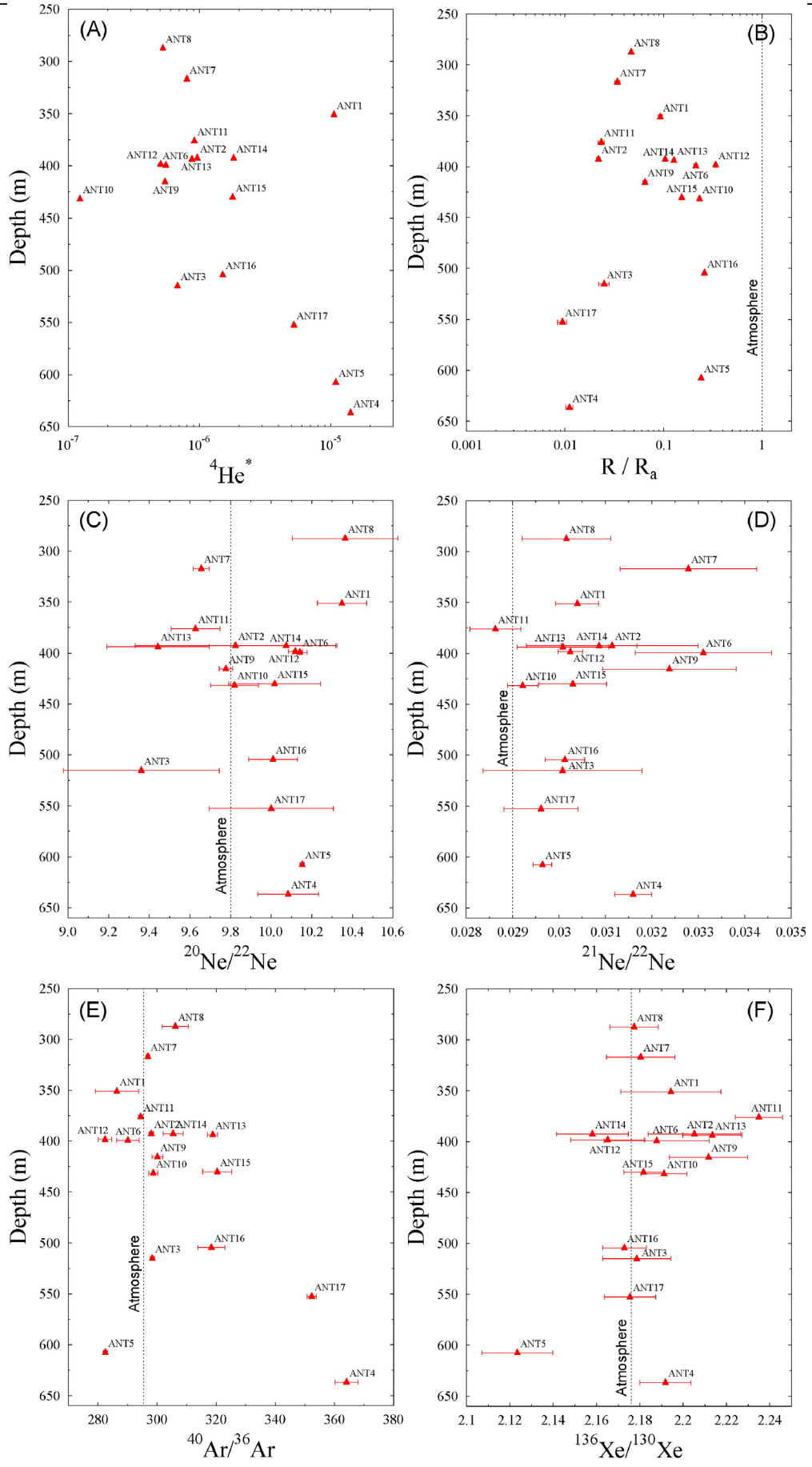
(A)
Depth (m)
$^4He^*$
(B)
R / R_a
Atmosphere
(C)
$^{20}Ne/^{22}Ne$
(D)
$^{21}Ne/^{22}Ne$
(E)
$^{40}Ar/^{36}Ar$
(F)
$^{136}Xe/^{130}Xe$
ANT1
ANT2
ANT3
ANT4
ANT5
ANT6
ANT7
ANT8
ANT9
ANT10
ANT11
ANT12
ANT13
ANT14
ANT15
ANT16
ANT17

Table 3
Noble gas isotopic volume fractions and calculated ^{4}He ages using representative values for only in-situ production, as well as both in-situ production and external He flux for Antrim Shale gas samples.

Sample ID	^{4}He ($\times10^{-7}$)	^{21}Ne ($\times10^{-12}$)	^{40}Ar ($\times10^{-6}$)	^{4}He* ($\times10^{-7}$)	^{21}Ne* ($\times10^{-13}$)	^{40}Ar* ($\times10^{-8}$)	^{136}Xe* ($\times10^{-12}$)	^{4}He ages without external flux ($\times10^5$ yr)	^{4}He ages with external flux ($\times10^3$ yr)
ANT1	106.71 ± 2.18	423.63 ± 5.51	28.23 ± 0.37	105.78 ± 2.16	199.23 ± 76.07	–	0.54 ± 2	18.22 ± 0.46	39.65 ± 1
ANT2	9.61 ± 0.14	9.55 ± 0.3	48.69 ± 0.63	9.61 ± 0.14	6.69 ± 3.83	50.56 ± 89.05	1.89 ± 4.4	1.02 ± 0.02	2.21 ± 0.04
ANT3	6.81 ± 0.1	9.38 ± 0.28	68.54 ± 0.89	6.8 ± 0.1	3.47 ± 3.48	78.65 ± 125.29	0.24 ± 5.9	0.51 ± 0.01	1.11 ± 0.02
ANT4	141.46 ± 2.12	13.98 ± 0.18	8.12 ± 0.11	141.62 ± 2.12	8.56 ± 2.69	154.38 ± 13.59	0.72 ± 3.06	109.43 ± 2.17	238.19 ± 4.73
ANT5	111.31 ± 1.67	10,721.98 ± 139.39	1338.63 ± 17.4	109.32 ± 1.64	2841.08 ± 1945.27	–	–	0.41 ± 0.01	0.88 ± 0.02
ANT6	5.65 ± 0.08	328.05 ± 4.26	51.84 ± 0.67	5.54 ± 0.08	410.61 ± 56.66	–	0.91 ± 5.19	0.55 ± 0.01	1.19 ± 0.02
ANT7	8.02 ± 0.12	93.89 ± 1.22	98.15 ± 1.28	8.02 ± 0.12	109.46 ± 16.29	65.09 ± 179.85	0.48 ± 7.1	0.42 ± 0.01	0.91 ± 0.02
ANT8	5.27 ± 0.08	16.65 ± 0.53	8.73 ± 0.11	5.26 ± 0.08	7.8 ± 6.59	32.06 ± 17.24	0.16 ± 6.93	3.19 ± 0.07	6.94 ± 0.15
ANT9	5.48 ± 0.08	46.76 ± 0.61	14.54 ± 0.19	5.45 ± 0.08	49.3 ± 8.16	25.13 ± 26.5	1.69 ± 3.22	1.95 ± 0.04	4.25 ± 0.08
ANT10	1.26 ± 0.02	5.61 ± 0.07	4.49 ± 0.06	1.23 ± 0.02	–	5.65 ± 8.21	1.34 ± 5.95	1.45 ± 0.03	3.15 ± 0.06
ANT11	9.14 ± 0.14	31.04 ± 0.59	84.25 ± 1.1	9.14 ± 0.14	–	–	3.83 ± 4.45	0.55 ± 0.01	1.2 ± 0.02
ANT12	5.22 ± 0.08	456.11 ± 5.93	59.42 ± 0.77	5.05 ± 0.08	181.24 ± 82.21	–	–	0.43 ± 0.01	0.93 ± 0.02
ANT13	8.88 ± 0.13	41.25 ± 1.34	13.78 ± 0.18	8.76 ± 0.13	–	55.42 ± 39.89	3.47 ± 6.3	3.42 ± 0.11	7.44 ± 0.23
ANT14	18.36 ± 0.28	28.39 ± 0.75	30.62 ± 0.4	18.17 ± 0.27	9.08 ± 10.13	105.34 ± 55.34	–	3.16 ± 0.06	6.88 ± 0.14
ANT15	18.19 ± 0.27	35.52 ± 0.84	13.29 ± 0.17	17.89 ± 0.27	8.07 ± 11.57	105.36 ± 26.18	0.36 ± 4.12	7.57 ± 0.17	16.48 ± 0.36
ANT16	15.49 ± 0.23	66.77 ± 0.89	14.94 ± 0.19	15.03 ± 0.23	–	109.88 ± 28.34	–	5.7 ± 0.12	12.4 ± 0.26
ANT17	52.27 ± 0.78	18.1 ± 0.48	8.38 ± 0.11	52.34 ± 0.79	1.91 ± 7.3	125.74 ± 25.23	–	37.34 ± 1.32	81.27 ± 2.87

However, irrespective of an atmospheric or mantle origin leading to slightly higher R/Ra values, the radiogenic ^{4}He component is largely dominant. For example, if He is treated as a two component mixture, a mantle and a crustal component, using a mantle R/Ra value of 8 and a crustal production value of 0.01 (Ballentine et al., 1991), crustal ^{4}He contributions in these samples vary between 96.8% and 100% of total measured ^{4}He, which strongly indicates the dominance of crustal He in Antrim gas samples. No obvious correlation is observed between R/Ra and depth (Fig. 3B). Typically, one would expect the R/Ra ratio to increase toward the surface due to incorporation of atmospheric He being carried by recharge water, leading to dilution of crustally produced He.

Some samples (e.g., ANT1, ANT8, ANT4, ANT5) also display ^{20}Ne/^{22}Ne ratios greater than the atmospheric value (9.8) which suggests the presence of some mantle Ne in these samples (Fig. 3C). ^{21}Ne/^{22}Ne ratios vary from 0.0286 ± 0.0005 to 0.0331 ± 0.0004 (Fig. 3D) reflecting the addition of crustally produced ^{21}Ne for samples with values greater than the atmospheric one (0.029) through the nuclear reactions of ^{18}O(α, n)^{21}Ne and ^{24}Mg(n, α)^{21}Ne (Wetherill, 1954). Ne isotopic ratios in the Antrim gas samples point to a largely dominant atmospheric ^{21}Ne contribution varying from 87.5% to 98.9% of total measured ^{21}Ne and a much smaller amount of crustal ^{21}Ne (^{21}Ne*) contribution ranging from 1.1% to 12.5%. No clear correlation between ^{21}Ne/^{22}Ne with depth is observed (see also Section 4.2).

Most Antrim Shale gas samples display ^{40}Ar/^{36}Ar ratios above the atmospheric value (295.5), reflecting the addition of radiogenic ^{40}Ar (^{40}Ar*, Fig. 3E). In contrast to R/Ra and Ne isotopic ratios where no apparent correlation is found with depth, ^{40}Ar/^{36}Ar ratios display an overall increase with depth. Similar to ^{4}He, excesses of ^{40}Ar are commonly observed in old crustal fluids due to natural decay of ^{40}K in the rock (Ballentine et al., 1991, 1994; Elliot et al., 1993). Atmospheric ^{40}Ar is also largely dominant varying from 81% to 99.3% of total measured ^{40}Ar. The presence of crustally produced ^{40}Ar (^{40}Ar*) is further discussed below. Some samples also display ^{136}Xe/^{130}Xe ratios above the atmospheric value (2.176), up to 2.235 ± 0.011, clearly showing the presence of excess crustally produced ^{136}Xe (Fig. 3F and Table 2). This excess ^{136}Xe was suggested to originate mainly from crustally produced ^{136}Xe from the spontaneous fission of ^{238}U in the Michigan Basin (Ma et al., 2009b). Unlike ^{40}Ar/^{36}Ar ratios, the highest ratios of ^{136}Xe/^{130}Xe are found at much shallower depths. From these observations it is apparent that noble gas isotopic ratios are highly variable with depth (Fig. 3).

Volume fractions of noble gas isotopes (^{4}He, ^{21}Ne and ^{40}Ar) and their crustally produced components in the Antrim Shale gas samples are reported in Table 3. Crustal He volume fractions (^{4}He*) in these Antrim gases are estimated by using the He isotopic ratios as discussed above (Fig. 3A). He is assumed to be essentially of crustal origin, while Ne, Ar and Xe are treated as a two-component mixture, with an atmospheric and a crustal end-member. Crustal ^{21}Ne, ^{40}Ar and ^{136}Xe contributions (^{21}Ne*, ^{40}Ar*, ^{136}Xe*) are estimated as follow (Ballentine, 1991):

$$^{21}\mathrm{Ne}* = {}^{21}\mathrm{Ne}_{\mathrm{measured}} \times \left(1 - \left(\frac{^{21}\mathrm{Ne}}{^{22}\mathrm{Ne}}\right)_{\mathrm{air}} / \left(\frac{^{21}\mathrm{Ne}}{^{22}\mathrm{Ne}}\right)_{\mathrm{measured}}\right) \quad (1)$$

$$^{40}\mathrm{Ar}* = {}^{40}\mathrm{Ar}_{\mathrm{measured}} \times \left(1 - \left(\frac{^{40}\mathrm{Ar}}{^{36}\mathrm{Ar}}\right)_{\mathrm{air}} / \left(\frac{^{40}\mathrm{Ar}}{^{36}\mathrm{Ar}}\right)_{\mathrm{measured}}\right) \quad (2)$$

$$^{136}\mathrm{Xe}* = {}^{136}\mathrm{Xe}_{\mathrm{measured}} \times \left(1 - \left(\frac{^{136}\mathrm{Xe}}{^{130}\mathrm{Xe}}\right)_{\mathrm{air}} / \left(\frac{^{136}\mathrm{Xe}}{^{130}\mathrm{Xe}}\right)_{\mathrm{measured}}\right) \quad (3)$$

where (^{21}Ne/^{22}Ne)$_{air}$ = 0.029, (^{40}Ar/^{36}Ar)$_{air}$ = 295.5 and (^{136}Xe/^{130}Xe)$_{air}$ = 2.176 (Ozima and Podosek, 2002). Calculated ^{21}Ne*, ^{40}Ar* and ^{136}Xe* are reported in volume fractions (Table 3). Neglecting the presence of a potentially minor mantle Ne, Ar and Xe contributions would not affect the discussion and conclusions that follow (Ma et al., 2009b).

^{4}He* volume fractions vary over two orders of magnitude, from 1.23×10^{-7} to 1.42×10^{-5} (Table 3). A plot of ^{4}He* versus depth (Fig. 3A) points to the presence of two groups, one at depths shallower than 450 m where no obvious correlation with depth is observed, the other at greater depths, displaying a correlation between ^{4}He* and depth (samples ANT3, ANT4, ANT5, ANT16 and ANT17). Overall, the high variability of ^{4}He* volume fractions with depth suggests variable in-situ radiogenic ^{4}He* production rates and/or variable external ^{4}He inputs. Fig. 4A, B displays the spatial distribution of volume fractions of total ^{4}He and ^{4}He* within the sampling area. Volume fractions of both total ^{4}He and ^{4}He* are identical with an overall increase from NW toward SE (samples ANT4 and ANT5). These identical distribution patterns and volume fractions suggest that ^{4}He* is the dominant component. Unlike total ^{4}He and ^{4}He*, spatial distributions of ^{21}Ne* (not shown) and ^{40}Ar* (Fig. 4D) differ greatly from that of total ^{21}Ne (not shown) and ^{40}Ar, respectively (Fig. 4C). This is expected since, as mentioned earlier, atmospheric ^{21}Ne and ^{40}Ar contents dominate total ^{21}Ne and ^{40}Ar volume fractions. ^{136}Xe* volume fractions vary from 1.60×10^{-13} to 3.83×10^{-12} (Table 3). No correlation is observed between ^{136}Xe* and depth. This is discussed below.

5. Discussion

Overall, multiple sources of noble gases (i.e., atmospheric, crustal, mantle) are present in the Antrim Shale. The contribution of each source varies significantly for different noble gases, e.g., total ^{4}He is dominated by crustally produced $^{4}He^{*}$ while $^{21}Ne^{*}$ and $^{40}Ar^{*}$ are relatively minor compared to corresponding atmospheric components. To assess whether or not such high variability in the noble gas signatures is caused by variable in-situ noble gas production from their parent elements (i.e., U, Th, ^{40}K) or instead due to variable contributions of the external flux into the Antrim Shale from deeper formations (brine migration) (Ma et al., 2005, 2009a; Walter et al., 1996), we evaluate below the extent of brine migration into the Antrim Shale.

5.1. Mixing of deep brine and freshwater recharge in the Antrim

Previous geochemical studies suggest that recharge (meteoric) water into the Antrim Shale accounts for 40%–80% of the co-produced water, with 20%–60% of co-produced water originating from deep brines, within the sampling area (McIntosh and Walter, 2005). In order to assess the impact of deep brines in each sampled Antrim well, we look at the measured $^{20}Ne/^{36}Ar$ ratios of the Antrim Shale gas samples.

^{36}Ar in sedimentary systems is almost entirely of atmospheric origin (Elliot et al., 1993; Ozima and Podosek, 2002). Similarly, Ne isotopes are predominantly of atmospheric origin with negligible ^{20}Ne mantle contributions in some of the samples (ANT1, ANT5, ANT6, ANT12,

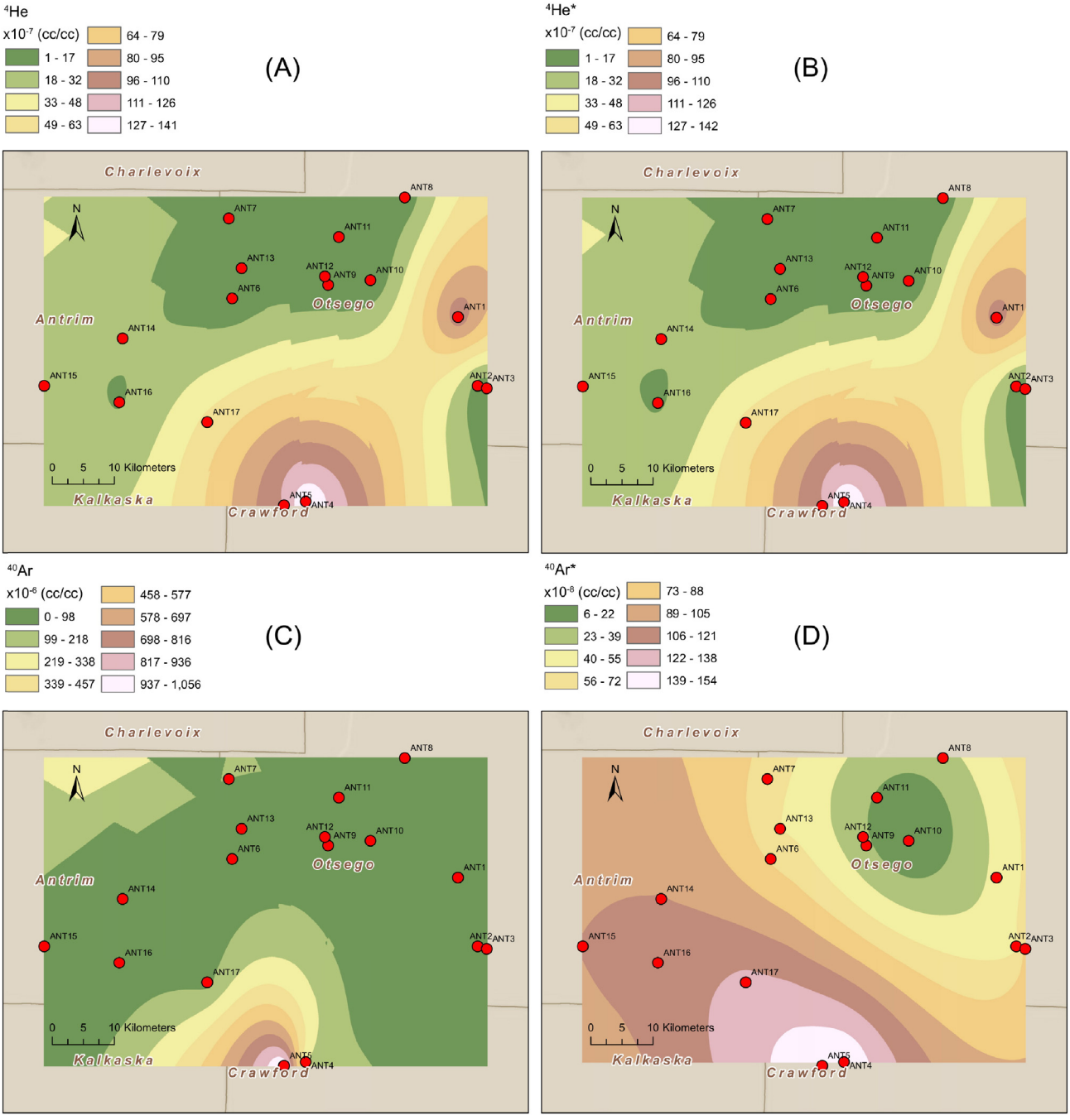

Fig. 4. Contour maps of (A) total ^{4}He volume fractions, (B) radiogenic ^{4}He volume fractions, (C) total ^{40}Ar volume fractions and (D) radiogenic ^{40}Ar volume fractions for Antrim Shale gas wells in this study.

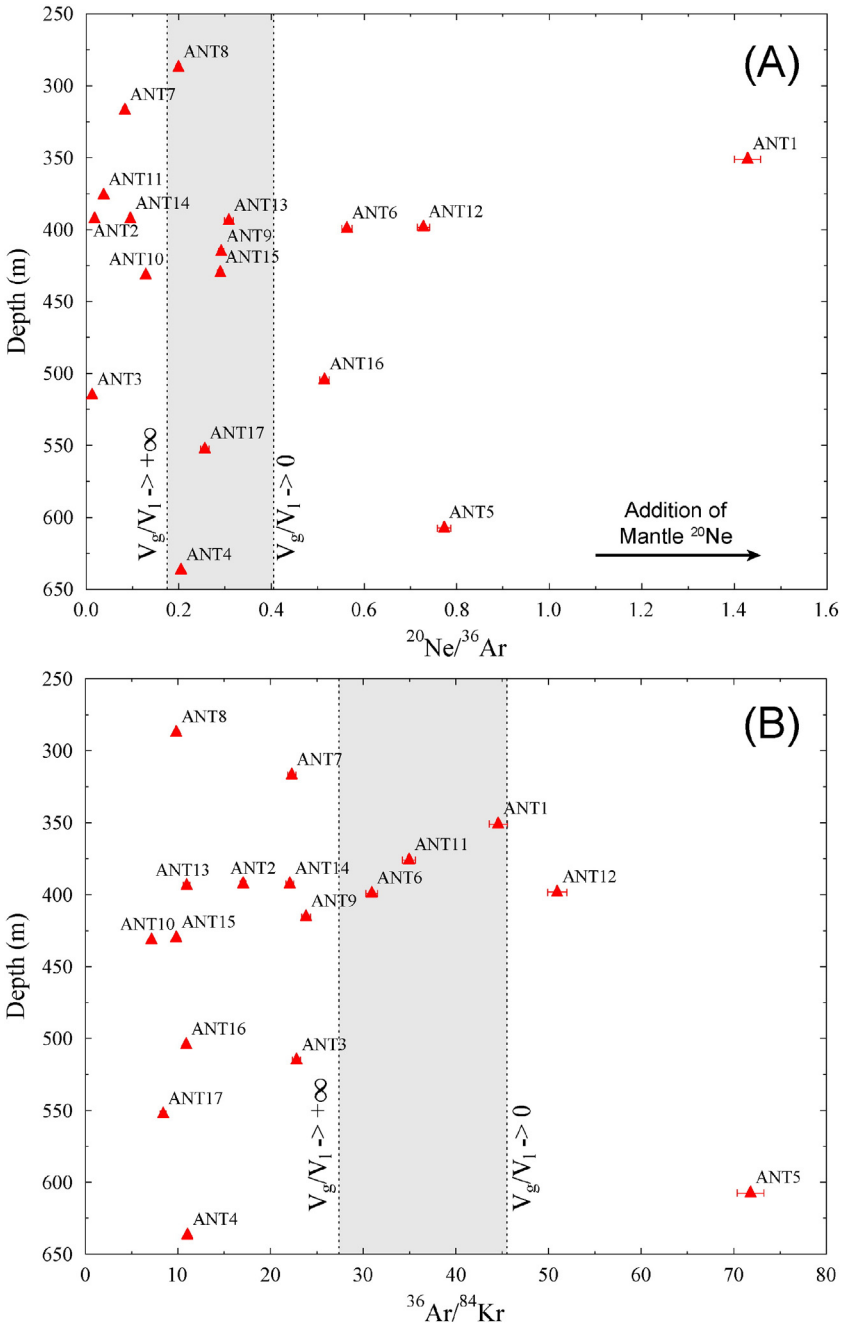

Fig. 5. Measured $^{20}Ne/^{36}Ar$ ratios of collected Antrim gas samples shown as a function of depth versus predicted $^{20}Ne/^{36}Ar$ ratios for a gas phase in equilibrium with seawater (i.e., gas/liquid volume ratio approaches 0 or $+\infty$) under reservoir conditions.

ANT16). In the analysis that follows, it is assumed that all ^{20}Ne and ^{36}Ar in the samples are of atmospheric origin. Atmospheric ^{20}Ne and ^{36}Ar components in the Antrim shale gases are assumed to originally derive from seawater with a salinity of 0.623 M in equilibrium with the atmosphere at 25 °C (Gutschick and Sandberg, 1991; Harrell et al., 1991), with $^{20}Ne/^{36}Ar = 0.175$ (Elliot et al., 1993; Ozima and Podosek, 2002). When a gas phase (e.g., CH_4) is present in contact with the water phase, $^{20}Ne/^{36}Ar$ ratios in the gas phase may be calculated if Henry's coefficients are known and a single-stage gas–liquid partitioning model is assumed (Elliot et al., 1993; Smith and Kennedy, 1983). Under current reservoir temperature of 24 °C and a water salinity of 5 M (Curtis, 2002; Hill and Nelson, 2000; Ma et al., 2009b; Martini et al., 1998), Ne and Ar Henry's coefficients are 458,314 and 197,872 atm, respectively (Crovetto et al., 1982; Smith and Kennedy, 1983). For a gas/liquid volume ratio (V_g/V_l) approaching 0, which is the maximum increase of ^{20}Ne volume fraction in the gas phase relative to the ^{36}Ar volume fraction under the single-stage gas–liquid equilibrium assumption, the predicted $^{20}Ne/^{36}Ar$ ratio in the gas phase is 0.405.

$^{20}Ne/^{36}Ar$ ratios (Table 2) of sampled Antrim gases are plotted in Fig. 5A and compared with $^{20}Ne/^{36}Ar$ ratios in the two extreme scenarios mentioned above, i.e., in which $V_g/V_l \rightarrow +\infty$ and 0. The first scenario represents the $^{20}Ne/^{36}Ar$ ratio (0.175) in the gas phase (left dashed line in Fig. 5A) assuming present-day reservoir conditions and V_g/V_l approaching $+\infty$, with all noble gases being transferred into the gas phase. The second scenario represents the $^{20}Ne/^{36}Ar$ ratio (0.405) in the gas phase (right dashed line in Fig. 5A) under current reservoir conditions assuming V_g/V_l approaching 0. In a closed system where the gas phase escapes from the liquid phase under variable gas/liquid volume

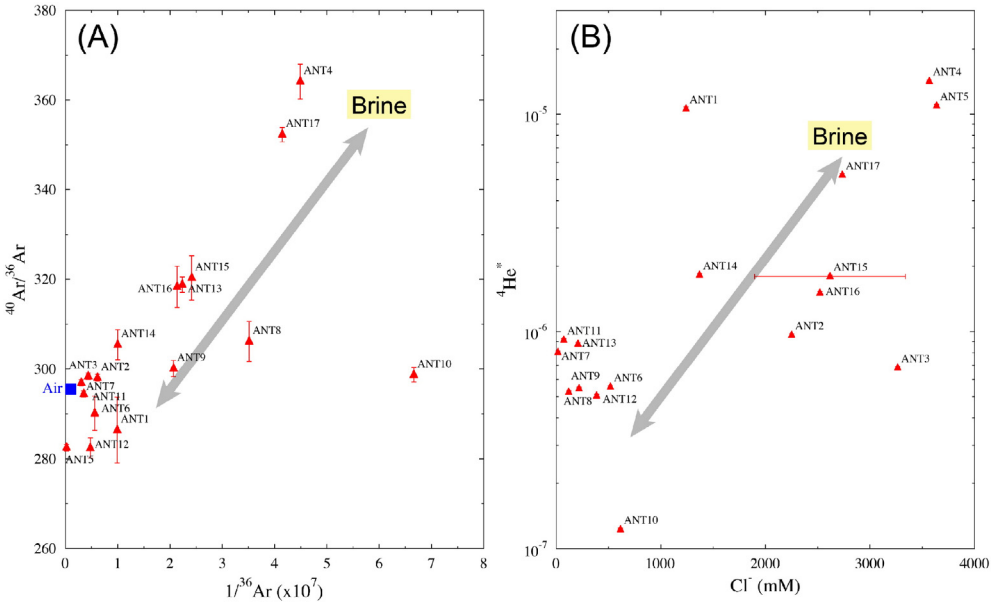

Fig. 6. (A) $^{40}Ar/^{36}Ar$ versus $1/^{36}Ar$; and (B) radiogenic ^4He volume fraction versus Cl^-. These reveal variable impact of deep brines on ^4He and Ar composition in the Antrim Shale.

ratios, all $^{20}Ne/^{36}Ar$ ratios in the gas phase (e.g., ANT8, ANT9, and ANT13) should fall within the range of 0.175–0.405 as shown by the gray domain region in Fig. 5A. However, two groups of Antrim gas samples are found outside of this gray domain. One group, comprising samples ANT1, ANT5, ANT6, ANT12 and ANT16 displays $^{20}Ne/^{36}Ar$ ratios higher than the predicted upper limit of 0.405 suggesting addition of mantle ^{20}Ne in the Antrim Shale other than the re-distribution of noble gases between the water and oil phases. It should be mentioned that the oil phase is scarce within the NPT area. In contrast, the second group, which includes samples ANT2, ANT3, ANT7, ANT10, ANT11 and ANT14, displays $^{20}Ne/^{36}Ar$ ratios which are lower than the $^{20}Ne/^{36}Ar$ ratio for $V_g/V_l \rightarrow +\infty$. These unusually low $^{20}Ne/^{36}Ar$ ratios in some of the Antrim Shale gas samples point to ^{20}Ne that is depleted relative to ^{36}Ar.

Similarly, ^{84}Kr is also almost entirely of atmospheric origin. $^{36}Ar/^{84}Kr$ ratios (Table 2) of sampled Antrim Shale gases are also plotted and compared with calculated $^{36}Ar/^{84}Kr$ ratios in the gas phase for the same two extreme scenarios (Fig. 5B). From Fig. 5B, it is apparent that $^{36}Ar/^{84}Kr$ ratios of most Antrim Shale gas samples are lower than the predicted minimum $^{36}Ar/^{84}Kr$ ratio in the gas phase ($V_g/V_l \rightarrow +\infty$), strongly indicating depletion of ^{36}Ar relative to ^{84}Kr. From Fig. 5A, B it is apparent that noble gas volume fractions of Antrim Shale gases display a mass-dependent depletion pattern with lighter noble gases being more heavily depleted compared to the heavier ones. A boiling model was suggested by Ma et al. (2009b) to explain such a mass-dependent depletion pattern in noble gas abundances from other formations in the Michigan Basin. This boiling model, proposed by Mazor and Truesdell (1984), describes the partitioning of noble gases between the water and steam phases according to Henry's Law. Atmospheric noble gas (e.g., ^{36}Ar) concentrations from the original seawater composition for both closed and open systems will leave the residual brine phase to the gas phase as boiling proceeds. Due to the higher solubility of the heavier noble gases (e.g., ^{84}Kr) compared to the lighter ones (e.g., ^{36}Ar) in brine, lighter noble gases will escape preferentially from the residual brine phase and will lead to mass-dependent depletion of noble gas in the brine. With the migration of deeper residual brines strongly depleted in noble gases into the Antrim Shale, noble gas from the residual brine will be transferred into the Antrim natural gas. Therefore, this mass-dependent depletion pattern will be observed in the Antrim gas samples we collected. This boiling model points strongly to the occurrence of past thermal events, which have been previously suggested to have occurred in the Michigan Basin (Castro et al., 2009; Coniglio et al., 1994; Fisher et al., 1988; Girard and Barnes, 1995; Ma et al., 2009a, 2009b; Sanford et al., 1985; Wang et al., 1994). Major thermal events in the Michigan Basin took place during the late Devonian-Mississippian (370–323 Ma), Triassic (~224 Ma) and Cretaceous (~111–159 Ma) related to the reactivation of the Precambrian basement structures. These are likely the cause of high paleo-temperatures (170–400 °C) in the Michigan Basin, which are thought to have ultimately led to the observed extreme depletion of atmospheric noble gases in the deep brines of the Michigan Basin. Occurrence of meteoric recharge water in the Antrim Shale is relatively recent and thought to have occurred during the Pleistocene and thus, far more recent than the occurrence of the past thermal events. Therefore, depletion of atmospheric noble gases would be expected to be found in old brines but not in the relatively young recharge water in the Antrim Shale. Volume fractions of atmospheric noble gases (e.g., ^{36}Ar) can be used to indicate the contribution of deep brines over the meteoric recharge water in the Antrim Shale gas.

Fig. 6A plots $^{40}Ar/^{36}Ar$ ratios of the Antrim Shale gas as a function of $1/^{36}Ar$ ratios. Both $^{40}Ar/^{36}Ar$ and $1/^{36}Ar$ ratios of the Antrim gas samples are highly variable, ranging from 282.4 to 364.1 and from 2.11×10^5 to 6.66×10^7 for $^{40}Ar/^{36}Ar$ and $1/^{36}Ar$ ratios, respectively. Such high variability is the result of variable contributions of old brine from deeper formations into the Antrim Shale mixing with recharge water. Unlike recharge water, deep brines come with high $^{40}Ar/^{36}Ar$ ratios due to crustally produced ^{40}Ar and higher $1/^{36}Ar$ ratios resulting from depletion of atmospheric noble gases which occurred during past thermal events (Ma et al., 2009b). Variable impact of the deep brines over recharge water can also be observed in the relationship displayed between $^4He^*$ and chloride concentrations in the co-produced water of the sampled wells (Fig. 6B). The chloride concentration of sampled co-produced formation water ranges from 16 to 3637 mM and the volume fractions of crustally produced $^4He^*$ vary over two orders of magnitude for the samples. Deep brines have higher salinity values (up to 5.7 M salinity, Wilson and Long, 1993a, 1993b) and more $^4He^*$ compared to meteoric water, although we cannot quantitatively evaluate brine and meteoric water end-members in our case due to the difficulty in comparing water and gas samples with respect to noble gas volume fractions. Samples ANT4 and ANT5 represent values close to the deep brine end members while ANT7, ANT10 and ANT11 are much closer to

Table 4
Calculated ^{4}He production rates in the Antrim Shale and the crust using representative values for estimated parameters.

Lithology	Thickness (m)	Porosity (%)	Th (ppm)	U (ppm)	Density (g/cm^3)	P(^{4}He)[a] (cm^3 STP g_{rock}^{-1} yr.$^{-1}$)
Antrim Shale[b]	95	9	1	20	2.7	2.71E−12
Upper Crust[c]	12,300	–	10.7	2.8	2.6	6.45E−13
Lower Crust[c]	36,900	–	1.06	0.28	3.3	6.42E−14

[a] Production rate of ^{4}He in the Antrim Shale, upper crust and lower crust. Please refer to the main text for detailed description.
[b] U and Th contents derived from Leventhal (1980) and Swanson (1960); thickness, porosity and density values after well logs (this study), Curtis (2002) and Clark (1966).
[c] U and Th contents derived from Taylor and McLennan (1985); thickness and density values after Ruff et al. (1994); Taylor and McLennan (1985) and Zhou and Ballentine (2006).

the recharge water end-member (He concentration and salinity are 5.1×10^{-8} cm^3 STP g^{-1} and 0 M Cl$^-$ at 0 °C, respectively).

It is apparent from the gas samples that large amounts of meteoric water recharged the Antrim Shale and mixed with variable amounts of old brines, which are derived from deep formations beneath the Antrim Shale and depleted in atmospheric noble gases (e.g., ^{36}Ar). Recharge of diluted meteoric waters likely stimulated microbial activity and the formation of biogenic methane in the Antrim Shale (Martini et al., 1996; Walter et al., 1996). It is thus critical to constrain both the origin of this recharge water as well as the timing of recharge.

5.2. ^{4}He groundwater ages

The accumulation of radiogenic ^{4}He (^{4}He*) has been widely used as a dating tool to constrain the age of groundwater beyond the ~50 ka limit of ^{14}C (Castro and Goblet, 2003; Castro et al., 2000; Ma et al., 2005; Schlegel et al., 2011; Torgersen and Clarke, 1985; Torgersen and Ivey, 1985; Wen et al., 2015). Water–gas interactions also result in the transfer of accumulated ^{4}He*, together with other dissolved atmospheric noble gases (e.g., ^{36}Ar), from the water to the gas phase (Ballentine, 1991; Zhou and Ballentine, 2006). The combined analyses of ^{4}He* and other noble gases allow us to estimate the accumulated ^{4}He* concentration in the water prior to the phase separation and thus, to acquire ^{4}He ages for the associated water phase (Schlegel et al., 2011; Zhou and Ballentine, 2006; Zhou et al., 2005).

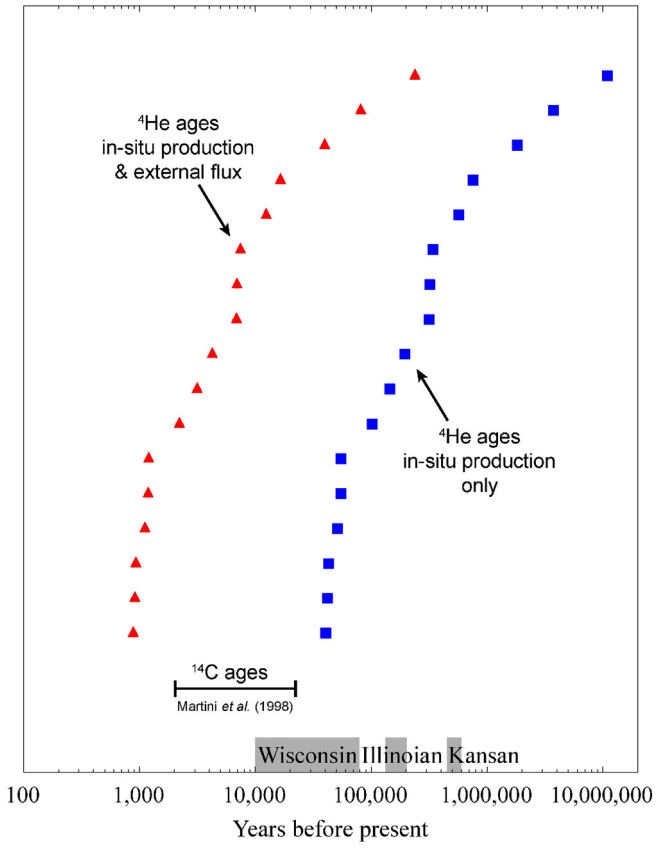

Fig. 7. Groundwater ^{4}He ages are shown for sampled Antrim wells in this study assuming: (a) only in-situ production (blue squares), and; (b) both in-situ production & external He flux (red triangles), and compared with previously reported groundwater ^{14}C ages (Martini et al., 1998) as well as timing of three major glacial periods (Wisconsin, Illinoian and Kansan) in the Michigan Basin.(For interpretation of the references to color in this figure legend, the reader is referred to the web version of this article.)

As discussed above, crustal ^{4}He dominates the total ^{4}He concentrations in the Antrim Shale gases, with minor amounts of mantle-derived and atmosphere-derived ^{4}He. The Antrim Shale samples display ^{4}He/^{20}Ne ratios ranging from 3 to 3099 (Table 2), which are much higher than the corresponding atmospheric ratio of 0.288 (Kipfer et al., 2002). High ^{4}He/^{20}Ne ratios also suggest minimal contamination of atmospheric He. Atmospheric noble gases are significantly depleted in deep brines which migrated into the Antrim Shale from deeper formations (Ma et al., 2009b). Past thermal events led to the decrease of atmospheric noble gas contents (e.g., ^{36}Ar) by a factor of ~100 (Ma et al., 2009b). Thus, most atmospheric noble gases (e.g., ^{36}Ar) in the Antrim are likely derived from relatively recent recharge water considering that contributions of meteoric water and brine are fairly equitable in the sampling area (McIntosh and Walter, 2005). ^{20}Ne/^{36}Ar and ^{36}Ar/^{84}Kr ratios of some Antrim Shale gases are out of the predicted ratio ranges for ASW (Fig. 5). However, considering the mixing of depleted deep brine and meteoric water, it is reasonable to assume that there has been minimal fractionation of the noble gases after the mixing of deep brine and meteoric water, with near complete transfer of noble gases from the water into the gas phase (Schlegel et al., 2011). Thus, all 17 Antrim Shale gas samples are used to calculate ^{4}He ages of associated formation water as a first-order estimation of the recharge timing in the Antrim Shale following Zhou and Ballentine (2006).

In the Antrim Shale, the major fraction of total ^{4}He is, by far, of radiogenic origin (^{4}He*), resulting from radioactive decay of U and Th both, within the Antrim Shale (in-situ production), and from ^{4}He produced at greater depths and migrating upwards with brine into the Antrim Shale. Thus, crustally produced ^{4}He* is given by (Schlegel et al., 2011):

$$^4\mathrm{He}* = {}^4\mathrm{He}_{\text{in-situ}} + {}^4\mathrm{He}_{\text{external}} \quad (4)$$

where ^{4}He$_{\text{in-situ}}$ and ^{4}He$_{\text{external}}$ represent the in-situ and externally produced ^{4}He, respectively.

Assuming that noble gases have been completely transferred from the associated water phase into the gas phase, ^{4}He concentrations in the water phase can be calculated based on ^{4}He and ^{36}Ar volume fractions in the gas phase as follows:

$$^4\mathrm{He}_{\text{water}} = \left(\frac{^4\mathrm{He}_{\text{measured}}}{^{36}\mathrm{Ar}_{\text{measured}}}\right)_{\text{air}} \times {}^{36}\mathrm{Ar}_{\text{ASW}} \quad (5)$$

where ^{36}Ar$_{\text{ASW}}$ represents the concentration of dissolved atmospheric ^{36}Ar in the water which is dependent on elevation, temperature and salinity of the recharge water. An average Ar concentration of 3.77×10^{-4} cm^3 STP g$^{-1}{}_{H2O}$ in the freshwater (0‰ salinity) at the temperature range of 0–25 °C and an elevation of 300 m (Gutschick and Sandberg, 1991; Harrell et al., 1991; Ma et al., 2004, 2005; Wen et al., 2015) is taken as the representative value of ^{36}Ar to calculate the ^{4}He concentrations in the water for each Antrim gas sample.

The in-situ production of ^{4}He is given by (Torgersen, 1980):

$$^4He_{in\text{-}situ} = P\left(^4He\right) \times \rho_r \times \Lambda \times \left(\frac{1-\omega}{\omega}\right) \times t \ \ cm^3STPg^{-1}{}_{H2O} \quad (6)$$

where ρ_r is the density of the rock in g cm^{-3}, t is the accumulation time (^{4}He age), ω is the porosity of the reservoir rock, Λ is the transfer efficiency of He from the rock matrix to the water, assumed to be 1 (Torgersen, 1980; Torgersen and Clarke, 1985), and P(^{4}He) is the in-situ production rate of ^{4}He within the Antrim Shale calculated by:

$$P\left(^4He\right) = 1.207 \times 10^{-13}[U] + 2.867 \times 10^{-14}[Th] \ \ cm^3STPg^{-1}{}_{rock}yr^{-1} \quad (7)$$

where [U] and [Th] represent the U and Th concentrations (in ppm), respectively (Table 4).

The external ^{4}He flux can be subsequently calculated by:

$$^4He_{external} = P\left(^4He\right) \times \rho_{crust} \times H \times \left(\frac{1}{\omega h}\right) \times t \ \ cm^3STPg^{-1}{}_{H2O} \quad (8)$$

where ρ_{crust} represents the density of the crust, H is the thickness of the crust in meters and h is the thickness of the Antrim Shale also in meters (Table 4).

^{4}He ages are calculated for two scenarios. In the first scenario, it is assumed that the Antrim Shale is a closed system and only in-situ ^{4}He has accumulated over geological times. The second scenario assumes that the Antrim Shale is an open system in which an average external ^{4}He flux migrated into the Antrim Shale and accumulated, in addition to the in-situ ^{4}He production. This external ^{4}He flux is partly supplied by underlying formations within the sedimentary sequence, partly from the crystalline basement in the Michigan Basin (Ma et al., 2005; Wen et al., 2015). In this contribution, we assume the upper crust and lower crust to be the source of this external ^{4}He flux (Table 4). Calculated ^{4}He ages using representative values (Table 4) for estimated parameters are listed in Table 3 and plotted in Fig. 7 for both scenarios. Considering only in-situ ^{4}He production, calculated ^{4}He ages range from 0.04 to 10.9 Ma (average 1.15 Ma), ages that are much younger than the formation age of the host rock (late Devonian is about 370 Ma). However, it has been shown that in most sedimentary basins, an external ^{4}He flux is present and must be accounted for in the calculation of groundwater ages (Castro and Goblet, 2003; Ma et al., 2005; Torgersen and Clarke, 1985; Wen et al., 2015; Zhou and Ballentine, 2006). More specifically, it was shown that a significant upward ^{4}He flux is present both at depth and in the shallow (shallower than the Antrim Shale) subsurface of the Michigan Basin (Castro et al., 2009; Ma et al., 2005, 2009a, 2009b; Wen et al., 2015). This external ^{4}He flux, from the upper and lower crust, is estimated at 3.33×10^{-9} cm^3 STP g$^{-1}{}_{H2O}$ in the Antrim Shale (Table 4). Accounting for the upward ^{4}He flux in the calculation of ^{4}He water ages in the Antrim Shale leads to water residence times ranging from 0.9 to 238.2 ka (average 25 ka), values which are on average younger by about two orders of magnitude than water ages considering a closed system (Fig. 7). Such large differences in these two sets of ^{4}He ages strongly suggest that in-situ ^{4}He production is minor compared to the external ^{4}He flux input in the Antrim Shale, which is present in shallower formations in the Michigan Basin (Ma et al., 2005; Wen et al., 2015). Comparing the ^{4}He ages with previously reported ^{14}C ages (Martini et al., 1998) for the Antrim Shale formation water (Fig. 7; Martini et al., 1998), we find that the latter, which vary from 2150 to 21,630 yrs., overlap with ^{4}He ages considering external ^{4}He input and further reinforce the notion that the Antrim Shale is an open system and that an external ^{4}He flux is present. Fig. 7 displays the timing of three major glaciation periods, i.e., Wisconsin (10 to 79 ka), Illinoian (132 to 202 ka) and Kansan (450 to 600 ka)

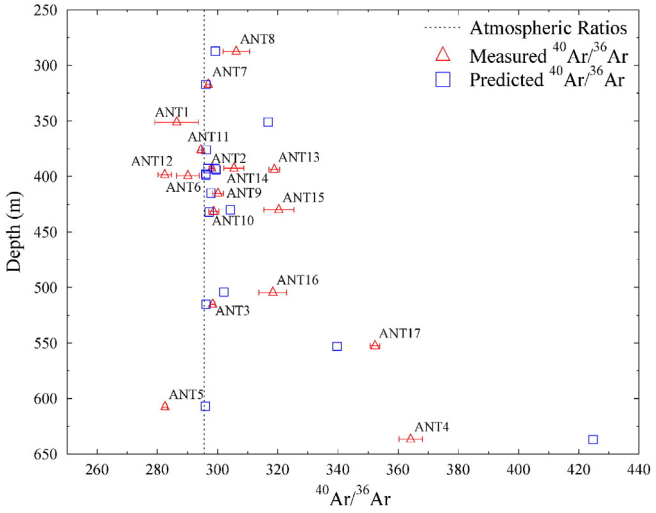

Fig. 8. Depth profiles versus (a) measured ^{40}Ar/^{36}Ar (red open triangles); and (b) predicted ^{40}Ar/^{36}Ar ratios (open blue square) for Antrim gas samples in this study. The atmospheric ^{40}Ar/^{36}Ar ratio is also indicated (dashed line). (For interpretation of the references to color in this figure legend, the reader is referred to the web version of this article.)

glaciations in the Michigan Basin (Bergquist, 2009; Dorr and Eschman, 1970; Schaetzl et al., 2008). Except for samples ANT15 and ANT17, open system calculated ^{4}He ages are within or younger than the Wisconsin glaciation period in the Michigan Basin. Samples ANT15 and ANT17 overlap with the Illinoian and Kansan glaciations (Fig. 7). These comparisons strongly suggest that Antrim Shale formation water in the study area was influenced to some extent by glaciation-associated meteoric recharge, the brines in the Antrim Shale may form from evaporated concentrated seawater which was subsequently modified by rock-water interactions at greater depths over geological time (Wilson and Long, 1993a, 1993b). Recharge of glacial meltwaters has been previously suggested based on geochemical evidence and numerical modeling studies (McIntosh and Martini, 2008; McIntosh et al., 2012; McIntosh and Walter, 2005) and shown to have close ties with the formation of biogenic methane in the Antrim Shale (Martini et al., 1996, 1998, 2003). As expected, calculated ^{4}He ages considering an external ^{4}He flux increase from NW to SE, following the observed ^{4}He* increase (Fig. 4B).

5.3. Differentiated Xe signatures relative to He, Ne and Ar

^{4}He formation water ages were obtained by accounting for the external ^{4}He flux entering the Antrim Shale (see Section 5.2). This external ^{4}He flux accounts for most radiogenic ^{4}He in the Antrim Shale relative to the negligible in-situ ^{4}He production. Similar findings are reported in shallower and deeper formations in the Michigan Basin (e.g., Saginaw Formation, Marshall Sandstone, Berea Sandstone, Traverse Group; cf. Fig. 1) (Ma et al., 2005, 2009a; Wen et al., 2015). In addition to ^{4}He flux, Ma et al., 2009a called upon an external ^{136}Xe flux to account for most of the measured crustally produced ^{136}Xe in the basin (e.g., Berea Sandstone and Traverse Group; Fig. 1). Ma et al. (2009a) also concluded that only the Precambrian crystalline basement can account for most of the measured crustally produced ^{4}He* and ^{136}Xe* in the Michigan Basin. Therefore a good correlation is expected between excess ^{4}He and excess ^{136}Xe. However, while ^{4}He* volume fractions show an overall correlation with depth, the same does not hold true for ^{136}Xe* (Fig. 3A, Table 3). This inconsistency between excess He and excess Xe can be explained by upward transport of crustal noble gases and associated elemental fractionation processes controlled by both diffusion- and solubility-related mechanisms (Ma et al., 2009a). High diffusivities and preferential volume fractions in the gas phase of He with respect to Xe lead to an enrichment of ^{4}He relative to ^{136}Xe in

shallower formations (i.e., the Antrim Shale) during upward transport. Relatively lower external ^{136}Xe abundance combined with the in-situ $^{136}Xe^*$ production from the ^{238}U spontaneous fission (Eikenberg et al., 1993) in the Antrim Shale may blur the correlation between $^{136}Xe^*$ and depth. On the other hand, $^{136}Xe^*$ volume fractions may reflect compositional variability within the Antrim Shale with respect to the radioactive parent (i.e., ^{238}U). According to Ma et al. (2009a), $^{40}Ar^*$ volume fractions should also be relatively depleted as compared to $^4He^*$ in the relatively shallow formation (i.e., the Antrim Shale) in the Michigan Basin. Thus no correlation should be observed between the $^{40}Ar^*$ volume fraction and depth. However, unlike $^{136}Xe^*$, $^{40}Ar^*$ has significant correlation with $^4He^*$ (not shown), which strongly points to the same external source, the Precambrian crystalline basement in the Michigan Basin, for both $^4He^*$ and $^{40}Ar^*$ components in the Antrim Shale. In addition to the in-situ crustally produced $^{136}Xe^*$ in the Antrim Shale, release of sedimentary Xe from the organic-rich black shale may also contribute to the total Xe composition in the Antrim Shale as previously suggested by Ma et al. (2009b); Podosek et al. (1980); Torgersen and Kennedy (1999) and Zhou et al. (2005). This contribution from sedimentary Xe may also dilute the $^{136}Xe^*$ and thus, may weaken the correlation between $^{136}Xe/^{130}Xe$ and depth (Fig. 3F). We note that the level that is most enriched in $^{136}Xe^*$ within the Antrim Shale is one of the shallowest, which might point to some local processes taking place. It is, however, premature at this stage to know with certainty the cause of this particular enriched layer in $^{136}Xe^*$. Additional samples with a wider spatial variability and depth need to be analyzed.

5.4. Origin of produced gases in the Antrim Shale: thermogenic versus biogenic origin

Produced hydrocarbon gases in the Antrim Shale consist of biogenic gases, which are associated with microbial activity stimulated by meteoric recharge through the well-developed fracture network in the Antrim Shale, as well as thermogenic gases, which were generated from cracking of oil or refractory kerogen (Martini et al., 1996; Stolper et al., 2014, 2015). However, the contribution of thermogenic methane with respect to the total produced methane in the study area is still under debate. Some early studies suggest that the thermogenic gas component contributes less than 20% of the total produced methane (Martini et al., 1996, 1998) while others argue for a more equal contribution of thermogenic and biogenic gases if not a dominating thermogenic component (Dolton and Quinn, 1996; Stolper et al., 2015). Below, we use noble gases as a tool to distinguish between thermogenic and biogenic methane and to assess their respective contributions in the study area.

We have shown that an external crustal ^4He flux is required to estimate the ages of Antrim Shale formation water. Similar to ^4He, ^{40}Ar also has external sources to the Antrim Shale (see, e.g., Ma et al., 2009a). If the radioelement composition in $^4He^*$ and $^{40}Ar^*$ source rock is assumed to be that of an average crustal composition with Th/U and K/U ratios of 3.8 and 1.2×10^4, respectively (Elliot et al., 1993; Taylor and McLennan, 1985), the radiogenic $^4He/^{40}Ar$ production ratio in the source formation will be 4.92 (Ballentine et al., 1991). The $^4He/^{40}Ar$ ratio of the external flux into the Antrim Shale will also be 4.92 assuming both that the subsurface temperature in the source rock is high enough to release all the Ar, i.e., ≥250 °C (Lippolt and Weigel, 1988; Pinti et al., 2011) and that no other processes have led to fractionation of the $^4He/^{40}Ar$ ratio (e.g., Castro et al., 1998a, 1998b). Given measured atmospheric-derived ^{36}Ar volume fractions and the atmospheric $^{40}Ar/^{36}Ar$ ratio of 295.5 (Ozima and Podosek, 2002), predicted $^{40}Ar/^{36}Ar$ ratios can be calculated assuming that Ar is fully released from the source formation (T > 250 °C) (Elliot et al., 1993):

$$\left(\frac{^{40}Ar}{^{36}Ar}\right)_{predicted} = \frac{^{36}Ar_{measured} \times 295.5 + {}^4He* /4.92}{^{36}Ar_{measured}}. \quad (9)$$

Predicted $^{40}Ar/^{36}Ar$ ratios are plotted in Fig. 8 together with measured $^{40}Ar/^{36}Ar$ ratios for all sampled Antrim Shale gases. The predicted $^{40}Ar/^{36}Ar$ over measured $^{40}Ar/^{36}Ar$ ratios are also listed in Table 2. The formation of thermogenic gases require reservoir temperatures between 157 and 221 °C, whereas biogenic gases yield formation temperatures consistent with their comparatively low-temperature formation environments (<50 °C) (Stolper et al., 2015), However this is lower than the Ar release temperature (250 °C) (Lippolt and Weigel, 1988). Given that predicted and measured $^{40}Ar/^{36}Ar$ ratios match well with each other, paleo subsurface temperatures in the source rock should be higher than the Ar release temperature and thus high enough for thermogenic methane formation. From the ratios of predicted over measured $^{40}Ar/^{36}Ar$, it is apparent that, with the exception of samples ANT1 and ANT4, all other Antrim gas samples have consistent measured and predicted $^{40}Ar/^{36}Ar$ ratio values, which tend to support that the contribution of thermogenic methane is greater than expected (<20%) in these samples. Stolper et al. (2015) established a mixing model of biogenic vs. thermogenic gases for Antrim Shale gases based on assumed formation temperatures of 18 °C and 144 °C for biogenic and thermogenic components, respectively. Their findings point to a larger proportion (~50%) of thermogenic gas in the Antrim Shale than previously thought. It is important to note that higher formation temperature of the thermogenic component in the mixing model will result in lower required amounts of the thermogenic gases. In our study, a greater formation temperature for thermogenic gas (>250 °C) is suggested. Even with this very high assumed temperature, their mixing model still suggests >25% thermogenic gases in the Antrim Shale. Thermal maturity of the Antrim Shale in the study area is relatively low and does not support in-situ production of thermogenic methane (Rullkötter et al., 1992), although the TOC content of the Antrim Shale is up to 24% (Martini et al., 1998). Therefore, thermogenic methane, as the major component of the total produced methane in the Antrim within the study area (NPT), must have an external origin. This external origin for the thermogenic methane might be either the portion of the Antrim Shale located in the deeper, central portion of the Michigan Basin or more deeply buried Silurian and older strata underlying the Antrim Shale (Stolper et al., 2015). Further work is required to distinguish these two external sources of thermogenic methane for Antrim Shale gas samples.

6. Conclusions

This study uses stable noble gases' (He, Ne, Ar, Kr, Xe) volume fractions and isotopic ratios from Antrim Shale gas samples to clarify vertical fluid migration, the occurrence of a past thermal event previously identified (Castro et al., 2009; Coniglio et al., 1994; Fisher et al., 1988; Girard and Barnes, 1995; Ma et al., 2009a, 2009b; Sanford et al., 1985; Wang et al., 1994), ages of formation water associated with natural gas, and to distinguish between thermogenic and biogenic methane in the Antrim Shale.

R/Ra ratios in Antrim Shale gas, where R is the measured $^3He/^4He$ ratio and Ra is the atmospheric ratio value of $1.384 \pm 0.013 \times 10^{-6}$, vary from an almost pure radiogenic (crustal) value of 0.009 ± 0.001 (typical crustal production values are ~0.01–0.05; Oxburgh et al., 1986), to 0.339 ± 0.006. Higher values of measured R/Ra ratios likely indicate the impact of mixing with an atmospheric component (R/Ra = 1) introduced during freshwater recharge. Crustal $^{21}Ne^*$, $^{40}Ar^*$ and $^{136}Xe^*$ contributions are also present but the atmospheric component is largely dominant for these gases. Crustal contributions for ^{21}Ne, ^{40}Ar and ^{136}Xe vary between 1.1% and 12.5%, between 0.7% and 19% and between 0.1% and 2.7%, respectively. Elevated $^{20}Ne/^{22}Ne$ ratios (up to 10.4) point to a minor mantle Ne component. High horizontal and vertical variability of noble gas signatures in the Antrim Shale are observed, which are due to variable noble gas input with brine migration from deeper formations and, to a smaller extent, are also due to variable in-situ production, in particular, the Lachine and Norwood members.

^{4}He ages are calculated for two scenarios: 1) the Antrim Shale is a closed system and only in-situ ^{4}He has accumulated over geological times; 2) the Antrim Shale is an open system and external ^{4}He flux migrated into the Antrim Shale and accumulated, in addition to the in-situ ^{4}He production. Considering only in-situ ^{4}He production, calculated ^{4}He ages range from 0.04 to 10.9 Ma (average 1.15 Ma), which are much older than ^{4}He ages of 0.9 to 238.2 ka (average 25 ka) considering both the upward external ^{4}He flux and in-situ ^{4}He production. Estimated ^{4}He ages considering external ^{4}He input for Antrim Shale water match well for most samples with the timing of the major Wisconsin glaciation (10 to 79 ka) in the Michigan Basin (Bergquist, 2009; Dorr and Eschman, 1970; Schaetzl et al., 2008), suggesting that Antrim Shale water was influenced by glaciation-induced recharge.

Given measured atmospheric-derived ^{36}Ar volume fractions and the atmospheric ^{40}Ar/^{36}Ar ratio of 295.5 (Ozima and Podosek, 2002), predicted ^{40}Ar/^{36}Ar ratios can be calculated assuming that Ar is fully released from the source formation (T > 250 °C) (Elliot et al., 1993). Measured and predicted ^{40}Ar/^{36}Ar ratios match well with each other for most Antrim Shale gases, indicating that paleo subsurface temperatures in the source rock should be higher than the Ar release temperature (250 °C) and thus high enough for thermogenic methane formation (157 and 221 °C) (Stolper et al., 2015). Thermal maturity of the Antrim Shale in the study area is relatively low and does not support in-situ production of thermogenic methane (Rullkötter et al., 1992), although the TOC content of the Antrim Shale is up to 24% (Martini et al., 1998). Therefore, thermogenic methane, which contributes most of the total produced methane in the Antrim within the study area, must originate from an external source. That might be either the deeper portion of the Antrim Shale located in the central Michigan Basin or more deeply buried Silurian and older strata underlying the Antrim Shale (Stolper et al., 2015).

Acknowledgments

We thank Prof. David Hilton for the editorial handling of this manuscript as well as Dr. Greg Holland and an anonymous reviewer for their insightful and thorough reviews. Financial support by the University of Michigan M-Cubed initiative U036713 and NSF awards 1049822 and CBET-1214416 is greatly appreciated. We also thank BreitBurn Energy Partners L.P. for access to their Antrim Shale gas wells as well as Phillip Brenz and Laura Bouvier for their assistance in the field.

References

Apotria, T., Kaiser, C.J., Cain, B.A., 1994. Fracturing and stress history of the Devonian Antrim Shale, Michigan basin. SPE Repr. Ser. 9–9.
Ballentine, C.J., 1991. He, Ne, and Ar Isotopes as Tracers in Crustal Fluids. Cambridge University Press.
Ballentine, C.J., Mazurek, M., Gautschi, A., 1994. Thermal constraints on crustal rare gas release and migration: evidence from Alpine fluid inclusions. Geochim. Cosmochim. Acta 58, 4333–4348.
Ballentine, C.J., O'nions, R.K., Oxburgh, E.R., Horvath, F., Deak, J., 1991. Rare gas constraints on hydrocarbon accumulation, crustal degassing and groundwater flow in the Pannonian Basin. Earth Planet. Sci. Lett. 105, 229–246. http://dx.doi.org/10.1016/0012-821X(91)90133-3.
Bergquist, S.G., 2009. The Glacial History and Development of Michigan. Michigan State University, pp. 1–12.
Boyer, C., Kieschnick, J., Suarez-Rivera, R., Lewis, R.E., 2006. Producing Gas From Its Source. Oilfield Review.
Castro, M.C., Goblet, P., 2003. Calibration of regional groundwater flow models: working toward a better understanding of site-specific systems. Water Resour. Res. 39. http://dx.doi.org/10.1029/2002WR001653 (1172–n/a).
Castro, M.C., Goblet, P., Ledoux, E., Violette, S., de Marsily, G., 1998a. Noble gases as natural tracers of water circulation in the Paris Basin: 2. Calibration of a groundwater flow model using noble gas isotope data. Water Resour. Res. 34, 2467–2483.
Castro, M.C., Jambon, A., de Marsily, G., Schlosser, P., 1998b. Noble gases as natural tracers of water circulation in the Paris Basin: 1. Measurements and discussion of their origin and mechanisms of vertical transport in the basin. Water Resour. Res. 34, 2443–2466.
Castro, M.C., Ma, L., Hall, C.M., 2009. A primordial, solar He–Ne signature in crustal fluids of a stable continental region. Earth Planet. Sci. Lett. 279, 174–184.
Castro, M.C., Stute, M., Schlosser, P., 2000. Comparison of 4He ages and 14C ages in simple aquifer systems: implications for groundwater flow and chronologies. Appl. Geochem. 15, 1137–1167.
Catacosinos, A.P., Daniels, P.A.J., 1991. Stratigraphy of Middle Proterozoic to Middle Ordovician formations of the Michigan Basin. Spec. Pap. Geol. Soc. Am. 53–71.
Cercone, K.R., Pollack, H.N., 1991. Thermal maturity of the Michigan Basin. Geol. Soc. Am. Spec. Pap. 256, 1–12.
Clark, S.P., 1966. Handbook of Physical Constants. Geological Society of America, New York.
Clark, J.A., 1982. Glacial Lading: A Cause of Natural Fracturing and a Control of the Present Stress State in Regions of High Devonian Shale Gas Production (SPE-10798-MS) http://dx.doi.org/10.2118/10798-MS.
Coniglio, M., Sherlock, R., Williams-Jones, A.E., Middleton, K., Frape, S.K., 1994. Burial and Hydrothermal Diagenesis of Ordovician Carbonates from the Michigan Basin, Ontario, Canada, in: Onlinelibrary (Wiley.com) Blackwell Publishing Ltd., Oxford, UK, pp. 231–254 http://dx.doi.org/10.1002/9781444304077.ch14.
Crovetto, R., Fernandez-Prini, R., Japas, M.L., 1982. Solubilities of inert gases and methane in H[sub 2]O and in D[sub 2]O in the temperature range of 300 to 600 K. J. Chem. Phys. 76, 1077–1086. http://dx.doi.org/10.1063/1.443074.
Curtis, J.B., 2002. Fractured shale-gas systems. AAPG Bull. 86, 1921–1938.
Darrah, T.H., Vengosh, A., Jackson, R.B., Warner, N.R., Poreda, R.J., 2014. Noble gases identify the mechanisms of fugitive gas contamination in drinking-water wells overlying the Marcellus and Barnett Shales. Proc. Natl. Acad. Sci. http://dx.doi.org/10.1073/pnas.1322107111.
Dolton, G.L., Quinn, J.C., 1996. An Initial Resource Assessment of the Upper Devonian Antrim Shale in the Michigan Basin. U S Geological Survey.
Dorr, J.A.J., Eschman, D.F., 1970. Geology of Michigan. University of Michigan, Ann Arbor.
Eikenberg, J., Signer, P., Wieler, R., 1993. U–Xe, U–Kr, and U–Pb systematics for dating uranium minerals and investigations of the production of nucleogenic neon and argon. Geochim. Cosmochim. Acta 57, 1053–1069.
Elliot, T., Ballentine, C.J., O'nions, R.K., Ricchiuto, T., 1993. Carbon, helium, neon and argon isotopes in a Po basin (northern Italy) natural gas field. Chem. Geol. 106, 429–440. http://dx.doi.org/10.1016/0009-2541(93)90042-H.
Farrand, W.R., Eschman, D.F., 1974. Glaciation of the southern peninsula of Michigan: a review. Mich. Academician 7, 31–56.
Fisher, J.H., Barratt, M.W., Droste, J.B., Shaver, R.H., 1988. Michigan Basin, in sedimentary cover-north American craton. Geol. Soc. Am. 361–382.
Girard, J.-P., Barnes, D.A., 1995. Illitization and paleothermal regimes in the middle Ordovician St. Peter sandstone, central Michigan Basin: K–Ar, oxygen isotope, and fluid inclusion data. AAPG Bull. 79, 49–69.
Graham, D.W., 2002. Noble gas isotope geochemistry of Mid-ocean ridge and ocean island basalts: characterization of mantle source reservoirs. Rev. Mineral. Geochem. 47, 247–317. http://dx.doi.org/10.2138/rmg.2002.47.8.
Gutschick, R.C., Sandberg, C.A., 1991. Late Devonian history of Michigan basin. Geol. Soc. Am. Spec. Pap. 256, 181–202.
Harrell, J.A., Hatfield, C.B., Gunn, G.R., 1991. Mississippian system of the Michigan Basin; stratigraphy, sedimentology, and economic geology. Geol. Soc. Am. Spec. Pap. 256, 203–220.
Harrison, W.B., 2007. Production history and reservoir characteristics of the Antrim shale gas play, Michigan Basin. AAPG East. Sect. Meet. 2007, 1-1.
Hill, D.G., Nelson, C.R., 2000. Gas Productive Fractured Shales — An Overview and Update: Gas Tips.
Hilton, D.R., Porcelli, D., 2003a. 2.06 — noble gases as mantle tracers. In: Turekian, H.D.H.K. (Ed.), Treatise on GeochemistryTreatise on Geochemistry. Pergamon, Oxford, pp. 277–318 http://dx.doi.org/10.1016/B0-08-043751-6/02007-7.
Hilton, D.R., Porcelli, D., 2003b. Noble gases as mantle tracers, in the mantle and core. In: Holland, H.D., Turekian, K.K. (Eds.), Treatise on Geochemistry. Elsevier, New York.
Hinze, W.J., Kellogg, R.L., O'Hara, N.W., 1975. Geophysical studies of basement geology of southern peninsula of Michigan. AAPG Bull. 59, 1562–1584.
Hunt, J.M., 1996. Petroleum Geochemistry and Geology. W H Freeman & Company.
Kipfer, R., Aeschbach-Hertig, W., Peeters, F., Stute, M., 2002. Noble gases in lakes and ground waters. Rev. Mineral. Geochem. 47, 615–700.
Kulongoski, J.T., Hilton, D.R., Izbicki, J.A., 2005. Source and movement of helium in the eastern Morongo groundwater basin: the influence of regional tectonics on crustal and mantle helium fluxes. Geochim. Cosmochim. Acta 69, 3857–3872. http://dx.doi.org/10.1016/j.gca.2005.03.001.
Leventhal, J.S., 1980. Comparative Geochemistry of Devonian Shale Cores from the Appalachian Basin, Mason, Monongalia, and Upshur Counties, West Virginia; Illinois Basin, Tazwell County, Illinois; Clark County, Indiana; and Michigan Basin, Sanilac County, Michigan. United States Geological Survey.
Lippolt, H.J., Weigel, E., 1988. 4He diffusion in 40Ar-retentive minerals. Geochim. Cosmochim. Acta 52, 1449–1458. http://dx.doi.org/10.1016/0016-7037(88)90215-3.
Ma, L., Castro, M.C., Hall, C.M., 2004. A late Pleistocene–Holocene noble gas paleotemperature record in southern Michigan. Geophys. Res. Lett. 31, L23204.
Ma, L., Castro, M.C., Hall, C.M., 2009a. Crustal noble gases in deep brines as natural tracers of vertical transport processes in the Michigan Basin. Geochem. Geophys. Geosyst. 10, Q06001.
Ma, L., Castro, M.C., Hall, C.M., 2009b. Atmospheric noble gas signatures in deep Michigan Basin brines as indicators of a past thermal event. Earth Planet. Sci. Lett. 277, 137–147.
Ma, L., Castro, M.C., Hall, C.M., Walter, L.M., 2005. Cross-formational flow and salinity sources inferred from a combined study of helium concentrations, isotopic ratios, and major elements in the Marshall aquifer, southern Michigan. Geochem. Geophys. Geosyst. 6, Q10004.
Manger, K.C., Oliver, S.J.P., Curtis, J.B., Scheper, R.J., 1991. Geologic influences on the location and production of Antrim Shale Gas, Michigan Basin (SPE-21854-MS) pp. 1–10.

Martini, A.M., Budai, J.M., Walter, L.M., Schoell, M., 1996. Microbial generation of economic accumulations of methane within a shallow organic-rich shale. Nature 383, 155–158. http://dx.doi.org/10.1038/383155a0.
Martini, A.M., Walter, L.M., Budai, J.M., Ku, T.C.W., Kaiser, C.J., Schoell, M., 1998. Genetic and temporal relations between formation waters and biogenic methane: upper Devonian Antrim Shale, Michigan Basin, USA. Geochim. Cosmochim. Acta 62, 1699–1720. http://dx.doi.org/10.1016/S0016-7037(98)00090-8.
Martini, A.M., Walter, L.M., Ku, T.C.W., Budai, J.M., McIntosh, J.C., Schoell, M., 2003. Microbial production and modification of gases in sedimentary basins: a geochemical case study from a Devonian shale gas play, Michigan basin. AAPG Bull. 87, 1355–1375. http://dx.doi.org/10.1306/031903200184.
Mazor, E., Truesdell, A.H., 1984. Dynamics of a geothermal field traced by noble gases: Cerro Prieto, Mexico. Geothermics 13, 91–102. http://dx.doi.org/10.1016/0375-6505(84)90009-9.
McIntosh, J.C., Martini, A.M., 2008. Chapter five: hydrogeochemical indicators for microbial methane in fractured organic-rich shales: case studies of the Antrim, New Albany, and Ohio Shales. pp. 162–174archives.datapages.com.proxy.lib.umich.edu.
McIntosh, J.C., Walter, L.M., 2005. Volumetrically significant recharge of Pleistocene glacial meltwaters into epicratonic basins: constraints imposed by solute mass balances. Chem. Geol. 222, 292–309.
McIntosh, J.C., Garven, G., Hanor, J.S., 2011. Impacts of Pleistocene glaciation on large-scale groundwater flow and salinity in the Michigan Basin. Geofluids 11, 18–33.
McIntosh, J.C., Schlegel, M.E., Person, M., 2012. Glacial impacts on hydrologic processes in sedimentary basins: evidence from natural tracer studies. Geofluids 12, 7–21. http://dx.doi.org/10.1111/j.1468-8123.2011.00344.x.
Menuge, J.F., Brewer, S.T., Seeger, C.M., 2002. Petrogenesis of metaluminous A-type rhyolites from the St. Francois Mountains, Missouri and the Mesoproterozoic evolution of the southern Laurentian margin. Precambrian Res. 269–291.
Nicot, J.-P., Scanlon, B.R., 2012. Water use for shale-gas production in Texas, U.S. Environ. Sci. Technol. 46, 3580–3586. http://dx.doi.org/10.1021/es204602t.
Nicot, J.-P., Scanlon, B.R., Reedy, R.C., Costley, R.A., 2014. Source and fate of hydraulic fracturing water in the Barnett shale: a historical perspective. Environ. Sci. Technol. 140206072907008. http://dx.doi.org/10.1021/es404050r.
Oxburgh, E.R., O'nions, R.K., Hill, R.I., 1986. Helium isotopes in sedimentary basins. Nature 324, 632–635. http://dx.doi.org/10.1038/324632a0.
Ozima, M., Podosek, F.A., 2002. Noble Gas Geochemistry. Cambridge University Press, New York.
Pinti, D.L., Marty, B., 1995. Noble gases in crude oils from the Paris Basin, France: implications for the origin of fluids and constraints on oil–water–gas interactions. Geochim. Cosmochim. Acta 59, 3389–3404. http://dx.doi.org/10.1016/0016-7037(95)00213-J.
Pinti, D.L., Marty, B., 2000. Noble gases in oil and gas fields: origins and processes. Fluids and Basin Evolution. Mineral Soc Can Short Course, pp. 160–196 (Chapter 7).
Pinti, D.L., Béland-Otis, C., Tremblay, A., Castro, M.C., Hall, C.M., Marcil, J.-S., Lavoie, J.-Y., Lapointe, R., 2011. Fossil brines preserved in the St-Lawrence Lowlands, Québec, Canada as revealed by their chemistry and noble gas isotopes. Geochim. Cosmochim. Acta 75, 4228–4243.
Pinti, D.L., Castro, M.C., Shouakar-Stash, O., Tremblay, A., Garduño, V.H., Hall, C.M., Hélie, J.F., Ghaleb, B., 2012. Evolution of the geothermal fluids at Los Azufres, Mexico, as traced by noble gas isotopes, δ18O, δD, δ13C and 87Sr/86Sr. J. Volcanol. Geotherm. Res. 249, 1–11.
Podosek, F.A., Honda, M., Ozima, M., 1980. Sedimentary noble gases. Geochim. Cosmochim. Acta 44, 1875–1884. http://dx.doi.org/10.1016/0016-7037(80)90236-7.
Porcelli, D., Ballentine, C.J., Wieler, R., 2002. An overview of noble gas geochemistry and cosmochemistry. Rev. Mineral. Geochem. 47, 1–19. http://dx.doi.org/10.2138/rmg.2002.47.1.
Price, L.C., Schoell, M., 1995. Constraints on the origins of hydrocarbon gas from compositions of gases at their site of origin. Nature 378, 368–371. http://dx.doi.org/10.1038/378368a0.
Ruff, L., LaForge, R., Thorson, R., Wagner, T., Goudaen, F., 1994. Geophysical Investigation of the Western Ohio–Indiana Region, Final Report 1986–1992. U.S. Nuclear Regulatory Commission: NUREG/CR-3145 10 p. 73.
Rullkötter, J., Marzi, R., Meyers, P., 1992. Biological markers in Paleozoic sedimentary rocks and crude oils from the Michigan Basin: reassessment of sources and thermal history of organic matter. In: Schidlowski, M., Golubic, S., Kimberley, M., McKirdy Sr., D., Trudinger, P. (Eds.), Early Organic Evolution. Springer Berlin Heidelberg, Berlin, Heidelberg http://dx.doi.org/10.1007/978-3-642-76884-2_25 (pp. 324–335–335).
Ryder, R.T., 1996. Fracture Patterns and Their Origin in the Upper Devonian Antrim Shale Gas Reservoir of the Michigan Basin.
Sanford, B.V., Thompson, F.J., McFall, G.H., 1985. Plate tectonics — a possible controlling mechanism in the development of hydrocarbon traps in southwestern Ontario. Bull. Can. Petrol. Geol. 33, 52–71.
Schaetzl, R.J., Darden, J.T., Brandt, D.S., 2008. Michigan Geography and Geology. Pearson Custom Pub.
Schlegel, M.E., Zhou, Z., McIntosh, J.C., Ballentine, C.J., Person, M.A., 2011. Constraining the timing of microbial methane generation in an organic-rich shale using noble gases, Illinois basin, USA. Chem. Geol. 287, 27–40. http://dx.doi.org/10.1016/j.chemgeo.2011.04.019.
Smith, S.P., Kennedy, B.M., 1983. The solubility of noble gases in water and in NaCl brine. Geochim. Cosmochim. Acta 47, 503–515. http://dx.doi.org/10.1016/0016-7037(83)90273-9.
Starkey, N.A., Stuart, F.M., Ellam, R.M., Fitton, J.G., Basu, S., Larsen, L.M., 2009. Helium isotopes in early Iceland plume picrites: constraints on the composition of high 3He/4He mantle. Earth Planet. Sci. Lett. 277, 91–100.
Stolper, D.A., Lawson, M., Davis, C.L., Ferreira, A.A., Neto, E.V.S., Ellis, G.S., Lewan, M.D., Martini, A.M., Tang, Y., Schoell, M., Sessions, A.L., Eiler, J.M., 2014. Formation temperatures of thermogenic and biogenic methane. Science 344, 1500–1503. http://dx.doi.org/10.1126/science.1254509.
Stolper, D.A., Martini, A.M., Clog, M., Douglas, P.M., Shusta, S.S., Valentine, D.L., Sessions, A.L., Eiler, J.M., 2015. Distinguishing and understanding thermogenic and biogenic sources of methane using multiply substituted isotopologues. Geochim. Cosmochim. Acta http://dx.doi.org/10.1016/j.gca.2015.04.015.
Swanson, V.E., 1960. Oil Yield and Uranium Content of Black Shales. United States Geological Survey.
Taylor, S.R., McLennan, S.M., 1985. The Continental Crust: Its Composition and Evolution. Wiley-Blackwell, Oxford.
Torgersen, T., 1980. Controls on pore-fluid concentration of 4He and 222Rn and the calculation of 4He/222Rn ages. J. Geochem. Explor. 13, 57–75. http://dx.doi.org/10.1016/0375-6742(80)90021-7.
Torgersen, T., Clarke, W.B., 1985. Helium accumulation in groundwater, I: an evaluation of sources and the continental flux of crustal 4He in the Great Artesian Basin, Australia. Geochim. Cosmochim. Acta 49, 1211–1218. http://dx.doi.org/10.1016/0016-7037(85)90011-0.
Torgersen, T., Ivey, G.N., 1985. Helium accumulation in groundwater. II: a model for the accumulation of the crustal 4He degassing flux. Geochim. Cosmochim. Acta 49, 2445–2452. http://dx.doi.org/10.1016/0016-7037(85)90244-3.
Torgersen, T., Kennedy, B.M., 1999. Air-Xe enrichments in Elk Hills oil field gases: role of water in migration and storage. Earth Planet. Sci. Lett. 167, 239–253. http://dx.doi.org/10.1016/S0012-821X(99)00021-7.
US EIA, 2015. Annual Energy Outlook 2015, eia.gov. US Energy Information Administration, Washington, DC.
Van Schmus, W.R., 1992. Tectonic setting of the midcontinent rift system. Tectonophysics 1–15.
Vugrinovich, R., 1986. Patterns of Regional Subsurface Fluid Movement in the Michigan Basin. United States Geological Survey, Lansing.
Walter, L.M., Budai, J.M., Abriola, L.M., Stearns, C.H., Martini, A.M., 1996. Hydrogeochemistry of the antrim shale northern Michigan basin. Annual report, September 1, 1993-May 1, 1995.
Wang, H.F., Crowley, K.D., Nadon, G.C., 1994. Thermal History of the Michigan Basin from Apatite Fission-Track Analysis and Vitrinite Reflectance.
Waples, D.W., 1985. Geochemistry in Petroleum Exploration. IHRDC.
Warrier, R.B., Castro, M.C., Hall, C.M., Lohmann, K.C., 2013. Large atmospheric noble gas excesses in a shallow aquifer in the Michigan Basin as indicators of a past mantle thermal event. Earth Planet. Sci. Lett. 375, 372–382. http://dx.doi.org/10.1016/j.epsl.2013.06.001.
Weiss, R.F., 1968. Piggyback sampler for dissolved gas studies on sealed water samples. Deep Sea Res. Oceanogr. Abstr. 15, 695–699.
Wen, T., Castro, M.C., Hall, C.M., Pinti, D.L., Lohmann, K.C., 2015. Constraining groundwater flow in the glacial drift and saginaw aquifers in the Michigan Basin through helium concentrations and isotopic ratios. Geofluids http://dx.doi.org/10.1111/gfl.12133 (n/a–n/a).
Westjohn, D.B., Weaver, T.L., 1996. Hydrogeologic framework of Mississippian rocks in the central Lower Peninsula of Michigan. Water-resources Investigations Report. United States Geological Survey.
Wetherill, G., 1954. Variations in the isotopic abundances of neon and argon extracted from radioactive minerals. Phys. Rev. 96, 679–683. http://dx.doi.org/10.1103/PhysRev.96.679.
Wilson, T.P., Long, D.T., 1993a. Geochemistry and isotope chemistry of CaNaCl brines in Silurian strata, Michigan Basin, U.S.A. Appl. Geochem. 8, 507–524. http://dx.doi.org/10.1016/0883-2927(93)90079-V.
Wilson, T.P., Long, D.T., 1993b. Geochemistry and isotope chemistry of Michigan Basin brines: Devonian formations. Appl. Geochem. 8, 81–100. http://dx.doi.org/10.1016/0883-2927(93)90058-O.
Zhou, Z., Ballentine, C.J., 2006. 4He dating of groundwater associated with hydrocarbon reservoirs. Chem. Geol. 226, 309–327.
Zhou, Z., Ballentine, C.J., Kipfer, R., Schoell, M., Thibodeaux, S., 2005. Noble gas tracing of groundwater/coalbed methane interaction in the San Juan Basin, USA. Geochim. Cosmochim. Acta 69, 5413–5428. http://dx.doi.org/10.1016/j.gca.2005.06.027.